



Calhoun: The NPS Institutional Archive
DSpace Repository

Theses and Dissertations

1. Thesis and Dissertation Collection, all items

1968-09

Echo Splitting in Linear FM Doppler Ranging Systems.

Cleary, Francis Paul

Monterey, California. Naval Postgraduate School

<http://hdl.handle.net/10945/40050>

This publication is a work of the U.S. Government as defined in Title 17, United States Code, Section 101. Copyright protection is not available for this work in the United States.

Downloaded from NPS Archive: Calhoun

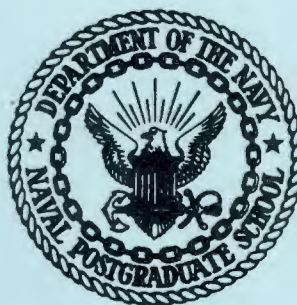


<http://www.nps.edu/library>

Calhoun is the Naval Postgraduate School's public access digital repository for research materials and institutional publications created by the NPS community. Calhoun is named for Professor of Mathematics Guy K. Calhoun, NPS's first appointed -- and published -- scholarly author.

Dudley Knox Library / Naval Postgraduate School
411 Dyer Road / 1 University Circle
Monterey, California USA 93943

UNITED STATES NAVAL POSTGRADUATE SCHOOL



THESIS

ECHO SPLITTING IN LINEAR FM
DOPPLER RANGING SYSTEMS

by

Francis Paul Cleary

September 1968

THESIS
C509

ECHO SPLITTING IN LINEAR FM
DOPPLER RANGING SYSTEMS

by

Francis Paul Cleary
//
Lieutenant, United States Navy
B.S., Naval Academy, 1962

Submitted in partial fulfillment of the
requirements for the degree of
MASTER OF SCIENCE IN ELECTRICAL ENGINEERING
from the

NAVAL POSTGRADUATE SCHOOL
September 1968

Signature of Author

Francis P. Cleary

Approved by

J. T. Hansen Jr.

Thesis Advisor

Charles H. Coltharp

Chairman, Department of Electrical Engineering

W. F. Koehler for R. F. Rinehart

Academic Dean

100
C.509
[REDACTED]
ABSTRACT

Echo splitting is a phenomenon that produces difficulties in estimating target range and speed for radar and sonar systems. It occurs when more than one returned pulse is received from a single target for each transmitted pulse. This thesis investigates the effects of echo-splitting distortion of a linear frequency modulated (chirp) signal. An ambiguity function is proposed for both narrow-band and wideband analysis of multiple and overlapping target returns. The double-echo situation is examined in detail and equations are developed for both the narrow-band and wideband cases. Finally, using typical sonar parameters, sample computer-drawn plots of these ambiguity functions are presented.

TABLE OF CONTENTS

Chapter	Page
I. INTRODUCTION	9
II. NARROW-BAND ANALYSIS	14
A. Background	14
B. Development of the Narrow-Band Ambiguity Function	16
C. Double-Echo Example	20
III. WIDEBAND ANALYSIS	29
A. Background	29
B. General Development of the Wideband Ambiguity Function	34
IV. DEVELOPMENT OF THE WIDEBAND AMBIGUITY FUNCTION FOR ECHO SPLITTING	37
A. System Model	37
B. Single-Return Development	42
C. Double-Echo Development	43
V. CONCLUSIONS	52
A. Summary	52
B. Areas of Future Study	52
BIBLIOGRAPHY	53
APPENDIX A. EXAMINATION OF THE NARROW-BAND AMBIGUITY FUNCTION FOR A PULSED CW SYSTEM UNDER MATCHED CONDITIONS.	54
APPENDIX B. EVALUATION OF THE WIDEBAND AMBIGUITY FUNCTION.	56

MO
VAN
DOD

LIST OF ILLUSTRATIONS

	Page
Fig. 1-1(a) Transmitted Pulse	10
Fig. 1-1(b) Matched Filter	10
Fig. 1-2 Underwater Multipaths	11
Fig. 1-3 Radar Multipath	12
Fig. 2-1 Envelope of the Output of a Matched Filter	19
Fig. 2-2 i^{th} Doppler Bank	19
Fig. 2-3 Narrow-Band Graph, Delay = .004	26
Fig. 2-4 Narrow-Band Graph, Delay = .010	27
Fig. 2-5 Narrow-Band Graph with Wideband Signal, Delay = .004	28
Fig. 3-1 Mismatched Signals: Narrow-Band Case	30
Fig. 3-2 Mismatched Signals: Wideband Case	31
Fig. 4-1 Envelope of the Output of a Matched Filter	38
Fig. 4-2 i^{th} Doppler Bank	38
Fig. 4-3 Envelope of Matched Filter Output	40
Fig. 4-4 i^{th} Doppler Bank	41
Fig. 4-5 Single-Return, Wideband Ambiguity Function	44
Fig. 4-6 Single-Return, Wideband Ambiguity Function	45
Fig. 4-7 Single-Return, Wideband Ambiguity Function	46
Fig. 4-8 Wideband Graph, Delay = .003	50
Fig. 4-9 Wideband Graph, Delay = .004	51

LIST OF PRINCIPLE SYMBOLS

$s_o(t)$	Transmitted Signal
$u(t)$	Unit Step Function
$X(t)$	Transmitted Pulse Envelope = $u(t) - u(t-T)$
$S_o(t)$	Complex Modulation Factor of Transmitted Signal
$r(t)$	Received Signal
$s'_{\omega_i}(t)$	Replica Signal with Assumed Doppler ω_i
$P(A, \tau, \omega)$	<u>a-posteriori</u> Probability of Detection
$P_o(A, \tau, \omega)$	<u>a-priori</u> Probability of Detection
N_o	Noise Power Density
I_o	Modified Bessel Function of the First Kind and Zero Order
$y(\tau, \omega)$	Output of a Matched Filter
$\psi(\tau, \omega)$	Ambiguity Function
T	Pulse Width
f_o	Carrier Frequency in Hz
ω_o	Carrier Frequency in radians/sec
ω_{d_j}	Doppler Frequency of j^{th} Reflector
t_{d_j}	Range Delay in Time of j^{th} Reflector
α_j	Relative Magnitude of Return of j^{th} Reflector
Δ	Time Delay Between Two Reflectors
B	Signal Bandwidth
c	Propagation Speed in the Medium
v_r	Radial Velocity
D	Doppler Factor
k	Rate of Frequency Sweep
μ	Rate of Radian Frequency Sweep

ACKNOWLEDGEMENT

I wish to take this opportunity to express my appreciation to Professor C. F. Klammer, Jr., who initially proposed this topic and greatly assisted me in its development.

CHAPTER 1

INTRODUCTION

The recognition of the science of signal processing has led to the initiation and development of a class of sophisticated pulse-type waveforms for communication systems. The fundamental property of this class is that each member signal possesses a large time-bandwidth product. The reception of such a signal by a cross-correlation detector produces time compression of the transmitted pulse. Selection of suitable transmitted waveform structures is called "signal waveform design." Systems utilizing correlation detection for signals having large time-bandwidth products are commonly said to employ "pulse compression techniques."

A pulse-compression technique that has found wide acceptance in radar and sonar applications is based upon a linear frequency modulated (LFM) pulse. In this technique, the carrier frequency is linearly swept to form a transmitted pulse of constant amplitude. The instantaneous frequency is expressed then as

$$f_0 + kt$$

during the pulse, where f_0 is the initial or carrier frequency. See Figure 1-1(a).

One method for implementing cross-correlation detection at the receiver is to use a linear filter whose transfer response to a unit impulsive input is the time inverse of the transmitted signal pulse. This is called a "matched filter detector." For LFM, the matched filter should have a constant gain characteristic over the required passband and a phase characteristic designed to provide a

linear time delay versus frequency plot, Figure 1-1(b). By retarding the leading portion of the received pulse waveform more than the trailing portion, the net effects of matched filter detection will be a compression in the time dimension of the filter output and an increase in the received signal amplitude.¹

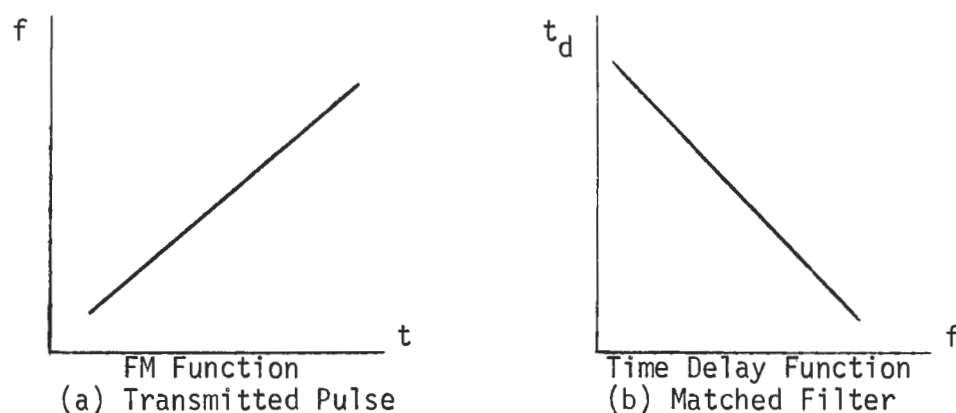


Fig. 1-1

LFM is both conceptually and technologically simple. The efficiency of operation of LFM systems has resulted in the continuing employment of this technique in advanced radar and sonar applications.

The ambiguity function, originally defined by P. M. Woodward,² examines the relative merits of a particular type of signal processing. It is a measure of the ability of a signal processing scheme to resolve two targets differing in range by a time delay τ and in doppler shift by frequency f' . But the ambiguity function can be interpreted in another manner. Rather than investigating the resolution between two targets, a replica of the transmitted signal is used at the receiver to simulate one target. Then the received signal is cross-correlated with this locally produced replica signal. W. M. Siebert has indicated that this cross-correlation of the received signal with a locally produced replica signal can be considered as the output of a matched filter.³ Consequently

the ambiguity function can be thought of as the envelope of the output of a matched filter, in the absence of noise, for a signal differing in range delay by a time τ and in frequency by f' .

It is the intent of this paper to investigate the ambiguity function of a linear FM signal in the presence of echo splitting. Echo splitting is a broad classification of two independent phenomena that cause distortion in the received signal.

The first of these is attributed to multipath transmission between source and target. Multipath manifests itself particularly in sonar systems where bottom bounce, surface reflection, and direct path propagation, and various combinations of these paths can illuminate the target. Figure 1-2 illustrates these paths by which illumination of the target can occur.

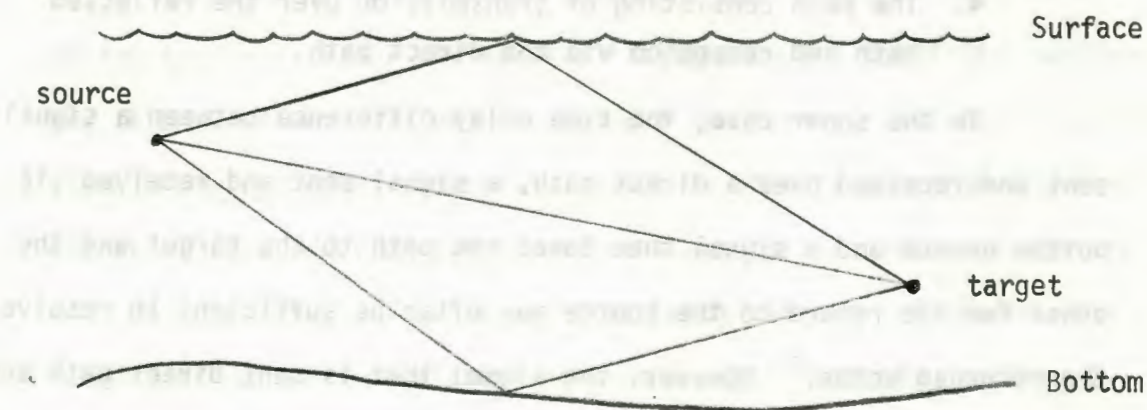


Fig. 1-2

Multipath is also found in certain radar applications and is especially noticeable in airborne radar.⁴ In this instance, a target can be illuminated by direct path and by surface reflection as shown in Figure 1-3.

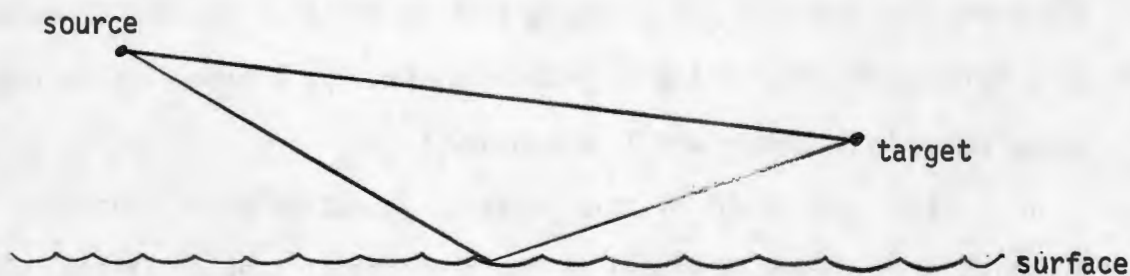


Fig. 1-3

The vagaries of both surface and bottom reflection will provide many paths between source and target. For this study, discussion will be limited to four paths:

1. A signal sent and received over a direct path.
2. A signal sent and received over a reflected path.
3. The path consisting of transmission over the direct path and reception via the reflected path.
4. The path consisting of transmission over the reflected path and reception via the direct path.

In the sonar case, the time delay difference between a signal sent and received over a direct path, a signal sent and received via bottom bounce and a signal that takes one path to the target and the other for its return to the source may often be sufficient to resolve the returned echos.⁵ However, the signal that is sent direct path and returns via bottom bounce will arrive in close proximity to a signal sent to the target via bottom bounce, and returned direct path. In a sonar system, separation between these two paths on the order of a few tens of milliseconds can be expected. Time separations of this order will produce difficulties in the detection problem.

The second cause of echo splitting is peculiar to sonar systems and is due solely to target dimensions. A sonar target is normally of

sufficient length, when compared to the length of a pulse, to display multiple reflecting surfaces. These individual reflection points will, depending on the aspect, present returns to the receiver sufficiently separated in time so as to cause distortion. The detection problem is further complicated by the possibility that the reflecting points can display different doppler shifts as in the case of a turning target.

There have been many developments of both narrow-band and, more recently, wideband ambiguity functions. In the narrow-band case, the assumption is made that the only effect of doppler on a transmitted signal is to shift the frequency components of the signal. This assumption neglects the effects of doppler distortion on the envelope or modulation. These effects will be shown to have considerable importance in wideband analysis.

Chapter II contains the development of a general narrow-band ambiguity function for the echo-splitting case. A model that explains how this function could be calculated is proposed. Finally, a specific example employing two returning signals is derived and computer-drawn graphs of this function are presented using typical sonar parameters.

In Chapter III, wideband considerations are introduced, and a simplified derivation of these effects on the ambiguity function is given.

Chapter IV proposes a system model based upon the wideband ambiguity function. An example with two returning signals is presented for the wideband case, and computer outputs are shown for various delays between the two signals.

Finally, Chapter V summarizes the results of this investigation, and suggests possible extensions of the work conducted in this thesis.

CHAPTER II

NARROW-BAND ANALYSIS

A. BACKGROUND

As previously mentioned, the work of Siebert best suits the initial phase of this investigation. Consequently, the following development is largely taken from that paper and is intended to clarify the symbols and expressions to be used.

In a linear FM system, the transmitted signal, $s_o(t)$, can be written as

$$s_o(t) = A\{u(t) - u(t-T)\} \cos(\omega_o t + \frac{1}{2} \mu t^2), \quad (2-1)$$

where

$$u(t) = \text{the unit step function} = \begin{cases} 1, & t > 0 \\ 0, & t < 0. \end{cases}$$

For ease of expression, we define

$$X(t) = u(t) - u(t-T),$$

so that Equation 2-1 is written

$$s_o(t) = A X(t) \cos(\omega_o t + \frac{1}{2} \mu t^2).$$

It is customary to normalize the energy level of the outgoing pulse by stating the condition that

$$\int_{-\infty}^{\infty} s_o^2(t) dt = 1. \quad (2-2)$$

Carrying out this operation reveals that the amplitude A of the pulse should be chosen as $\sqrt{\frac{2}{T}}$.

The transmitted signal can also be written in a canonic form, in this case as the real part of a complex signal. Thus

$$s_o(t) = \text{Re}[S_o(t) e^{j\omega_o t}];$$

where

$$S_o(t) = X(t) |S_o(t)| e^{j\frac{1}{2}\mu t^2}.$$

The complex modulation factor $S_0(t)$ must conform to the normalization of Equation 2-2:

$$|S_0(t)| = A = \sqrt{\frac{2}{T}}$$

In the narrow-band case, a returning signal, delayed by an amount τ and frequency shifted by ω_d can be written as

$$s_{\omega_d}(t-\tau) = \text{Re}[S_{\omega_d}(t-\tau) e^{j\omega_0(t-\tau)}],$$

where

$$S_{\omega_d}(t-\tau) = \alpha X(t-\tau) |S_0(t-\tau)| e^{j[\omega_d(t-\tau) + \frac{1}{2} \mu(t-\tau)^2]}.$$

In this last expression, α is introduced to express the amplitude of the received signal as a percentage of the normalized transmitted signal.

In the case of echo splitting, the received signal is a sum of the N returning echoes. It can be written as

$$r(t) = \sum_{j=1}^N \alpha_j s_{\omega_{d_j}}(t-t_{d_j}), \quad (2-3)$$

where t_{d_j} is the range delay, ω_{d_j} is the frequency change, and α_j is the relative amplitude of the j^{th} reflector.

It is necessary at this point to digress somewhat in order to give a short justification for the present approach. At first glance, it appears that the normal method of testing to see if two returning signals can be resolved will prove not only simpler but also more enlightening. For example, in the case of a target with two returns, the usual approach is to compare the ambiguity function of one return with that of the other return. If the two curves intersect below the 3db points, then the two targets are said to be resolvable. That is, an operator should be able to distinguish two targets.

But this is not the problem treated in this paper. The multiple returns that arrive with different delays, hence different phases, add together in the matched filter. Therefore, if an ambiguity function

can be developed utilizing these considerations, it could possibly suggest means of target identification and recognition. Such a possibility argues strongly for an effort in this direction, particularly in the sonar environment.

B. DEVELOPMENT OF THE NARROW-BAND AMBIGUITY FUNCTION

Siebert developed the relationship between the a-posteriori probability of detection, $P(A, \tau, \omega)$, and the a-priori probability, $P_0(A, \tau, \omega)$, as

$$P(A, \tau, \omega) = K P_0(A, \tau, \omega) e^{\frac{1}{N_0} \int_{-\infty}^{\infty} r(t) s'_{\omega_i}(t-\tau) dt} e^{-\frac{A^2}{N_0}} \quad (2-4)$$

For a single echo, τ and ω represent the range delay and doppler frequency mismatch between the received signal $r(t)$ and the replica of the transmitted signal $s'_{\omega_i}(t-\tau)$. N_0 is the noise power density in watts/Hz and K is a normalization constant. It is obvious from Equation 2-4, that the integral

$$\Lambda = \int_{-\infty}^{\infty} r(t) s'_{\omega_i}(t-\tau) dt \quad (2-5)$$

contains all the information that is necessary in the detection process.

It is also obvious that with the proper selection of the factor $s'_{\omega_i}(t-\tau)$, Equation 2-5 is simply the output of a matched filter. This integral will, however, contain the rapid variations of the fine structure of the signal caused by the carrier phase term, $\omega_0 \tau$. The fine structure does not in any way aid in the determination of the range of the target. For, although it is possible to determine in which fraction of the wavelength the target is located, there is no way to predict at which particular half-wavelength this occurs.

Siebert solved the problem in the narrow-band case by treating the $\omega_0 \tau$ term in $s'_{\omega_i}(t-\tau)$ as a random variable, θ , uniformly distributed

in the interval $0 \leq \theta \leq 2\pi$. Performing this operation on Equation 2-4, he arrived at the expression

$$\bar{P}(A, \tau, \omega) = KP(A, \tau, \omega) e^{-\frac{A^2}{2N_0}} I_0\left(\frac{A\Lambda_1}{N_0}\right),$$

where

I_0 is the modified Bessel function of the first kind and zero order and

$$\Lambda_1 = \left| \int_{-\infty}^{\infty} r(t) S'_{\omega_1}(t-\tau) e^{j\omega_0 t} dt \right|. \quad (2-6)$$

This operation has the result of essentially taking the envelope in the τ domain, of the expression in Equation 2-5. Equation 2-6 will be used as the basis for defining the ambiguity function ψ . For a multiple echo return, let

$$\psi(\tau, \omega) = \left| \int_{-\infty}^{\infty} r(t) S'_{\omega_1}(t-\tau) e^{j\omega_0 t} dt \right|,$$

where now τ and ω are multidimensional and must be carefully interpreted.

Equation 2-6 differs from Siebert's ambiguity function in that the carrier frequency phasor, $e^{j\omega_0 t}$, is retained. The necessity for keeping the carrier frequency can best be explained by consideration of a continuous-wave (cw) pulsed transmitter system. If two point reflectors are separated, for example, by a distance $\frac{\lambda}{4}$, then the received signal would essentially vanish since the total path difference is $\frac{\lambda}{2}$. Similarly, for a separation of $\frac{\lambda}{2}$, resulting in a total path difference of λ , the received signal would be doubled. Consequently, we might

expect that

$$\psi(0,0) \approx 0 \text{ for a total path difference of } \frac{\lambda}{2}$$

$$\psi(0,0) \approx 2 \text{ for a total path difference of } \lambda.$$

It is possible to hypothesize an equation to meet these conditions.

By defining the time for the wave to travel the round-trip distance between the two reflectors as Δ , then for

$$c\Delta = \frac{\lambda}{2}$$

$$\Delta = \frac{\pi}{\omega_0},$$

the result is

$$\psi(0,0) = 0.$$

Also, for

$$c\Delta = \lambda$$

$$\Delta = \frac{2\pi}{\omega_0},$$

then

$$\psi(0,0) = 2.$$

It is easy to see that

$$\psi(0,0) = 2 \left| \cos \frac{\omega_0 \Delta}{2} \right|$$

satisfies these conditions. Appendix A shows that for the case of two point reflectors, Equation 2-6 leads to this expression for $\psi(0,0)$.

The carrier frequency phasor is thus an important factor in ambiguity functions pertaining to signals in an echo-splitting environment.

Before continuing, it is appropriate to indicate just how this function might be generated in practice. Figure 2-1 is one possible block diagram for a matched filter system that is suitable for narrow-band considerations. Figure 2-2 is a breakdown of a particular doppler

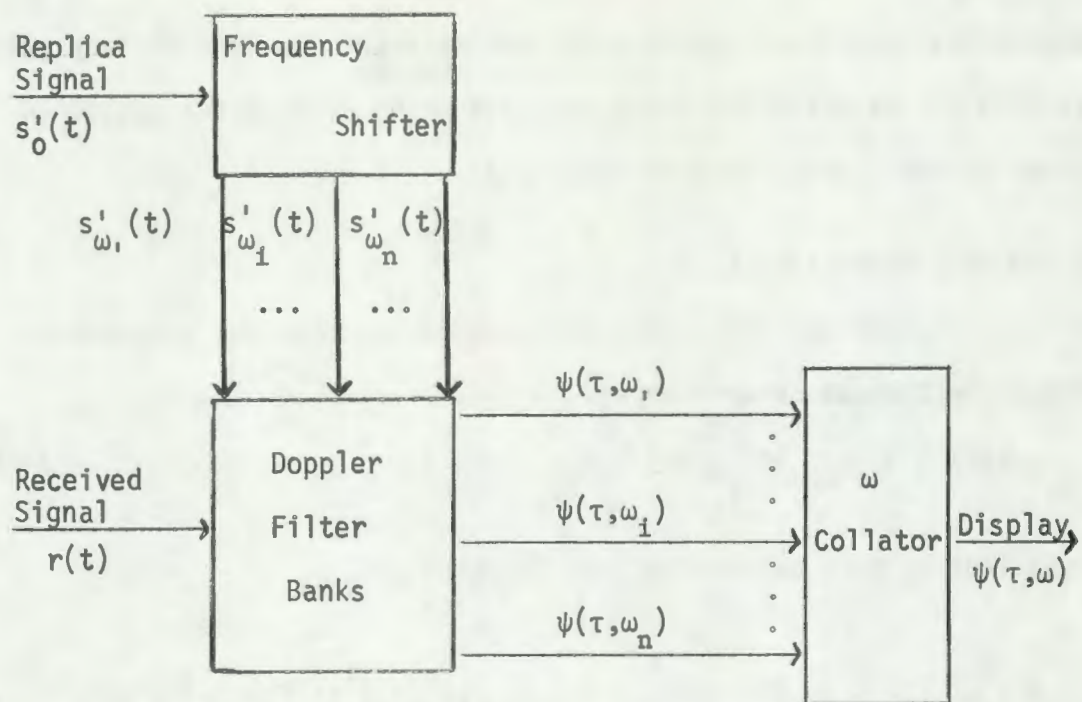


Fig. 2-1 ENVELOPE OF THE OUTPUT OF A MATCHED FILTER

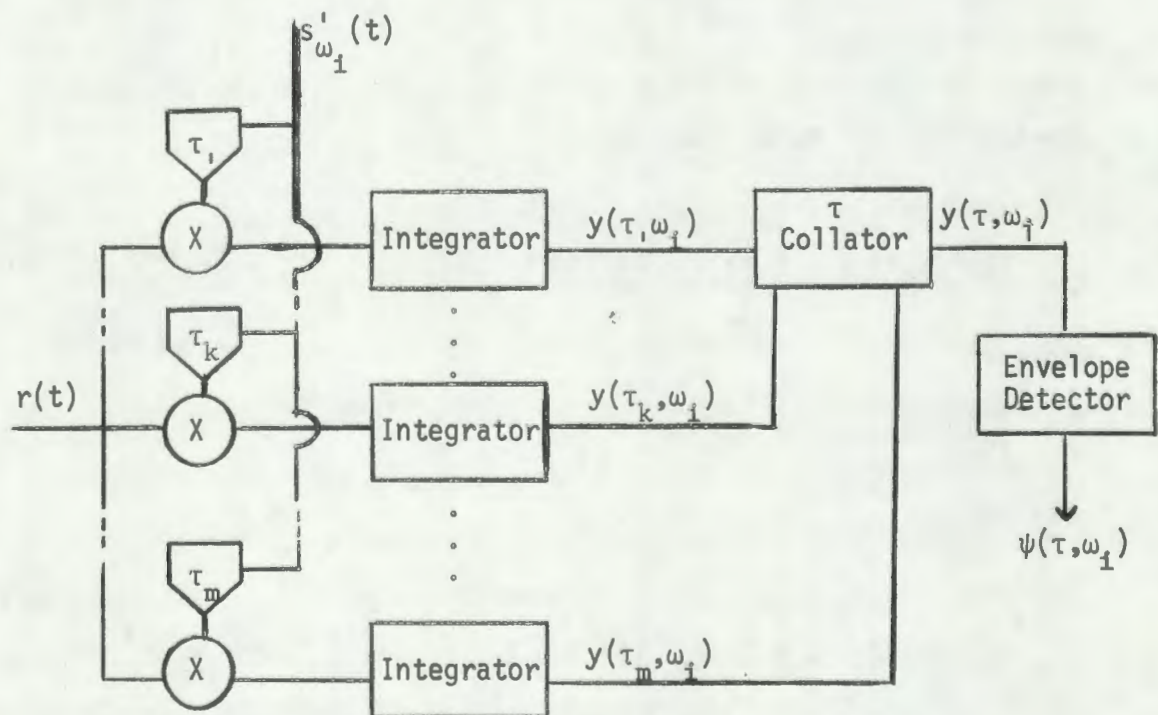


Fig. 2-2 i^{th} DOPPLER BANK

bank. The functional blocks entitled "collator" collect the various outputs for each shifted value of τ and ω and arrange the values in order on the τ and ω axes respectively.

C. DOUBLE-ECHO EXAMPLE

If only two reflectors are considered, then the received signal, $r(t)$, can be written as

$$r(t) = \alpha_1 s_{\omega_{d_1}}(t-t_{d_1}) + \alpha_2 s_{\omega_{d_2}}(t-t_{d_2}). \quad (2-7)$$

Substituting this expression into Equation 2-6,

$$\psi(\tau, \omega) = \left| \int_{-\infty}^{\infty} [\alpha_1 s_{\omega_{d_1}}(t-t_{d_1}) + \alpha_2 s_{\omega_{d_2}}(t-t_{d_2})] S'_{\omega_i}(t-\tau) e^{j\omega_0 t} dt \right|. \quad (2-8)$$

By defining

$$t' = t - t_{d_1},$$

$$\Delta = t_{d_2} - t_{d_1},$$

and $\tau' = \tau - t_{d_1},$

Equation 2-8 can be written as

$$\psi(\tau', \omega, \Delta) = \left| \int_{-\infty}^{\infty} [\alpha_1 s_{\omega_{d_1}}(t') + \alpha_2 s_{\omega_{d_2}}(t' - \Delta)] S'_{\omega_i}(t' - \tau') e^{j\omega_0 t'} e^{j\omega_0 t_{d_1}} dt' \right|.$$

Since

$$|e^{j\omega_0 t_{d_1}}| = 1,$$

this becomes

$$\psi(\tau', \omega, \Delta) = \left| \int_{-\infty}^{\infty} [\alpha_1 s_{\omega_{d_1}}(t) + \alpha_2 s_{\omega_{d_2}}(t - \Delta)] S'_{\omega_i}(t - \tau') e^{j\omega_0 t} dt \right|. \quad (2-9)$$

In Equation 2-9, the dummy variable of integration t' is replaced by t . From the above substitutions, it is seen that Δ is simply the difference in arrival time between the two returns. Thus, Equation 2-7 could have been written as

$$r(t) = \alpha_1 s_{\omega_{d_1}}(t) + \alpha_2 s_{\omega_{d_2}}(t-\Delta),$$

although it should be noted that the ambiguity function is now plotted as a function of τ' which is shifted from the original τ origin by the time delay of the first return.

For a linear FM signal, Equation 2-9 is written as

$$\psi(\tau', \omega, \Delta) = \frac{2}{T} \left| \int_{-\infty}^{\infty} \left[\alpha_1 X(t) \cos \{(\omega_0 + \omega_{d_1})t + \frac{1}{2}\mu t^2\} + \alpha_2 X(t-\Delta) \right. \right. \\ \left. \left. \cdot \cos \{(\omega_0 + \omega_{d_2})(t-\Delta) + \frac{1}{2}\mu(t-\Delta)^2\} \right] X(t-\tau') e^{j[\omega_1(t-\tau') + \frac{1}{2}\mu(t-\tau')^2 + \omega_0 t]} dt \right|. \quad (2-10)$$

By applying appropriate trigonometric identities, Equation 2-10 can be written in the form

$$\psi(\tau', \omega, \Delta) = \frac{\alpha_1}{T} \int_{x_1}^{x_2} \left\langle \cos x + \cos y + j \sin x + j \sin y \right\rangle dt \\ + \frac{\alpha_2}{T} \int_{x_3}^{x_4} \left\langle \cos z + \cos v + j \sin z + j \sin v \right\rangle dt \Big|, \quad (2-11)$$

where

$$x = \mu t^2 + (2\omega_0 + \omega_1 + \omega_{d_1} - \mu\tau')t + \frac{1}{2}\mu\tau'^2 - \omega_1\tau'$$

$$y = (\omega_1 - \omega_{d_1} - \mu\tau')t + \frac{1}{2}\mu\tau'^2 - \omega_1\tau'$$

$$z = \mu t^2 + (2\omega_0 + \omega_1 + \omega_{d_2} - \mu\{\tau' - \Delta\})t + \frac{1}{2}\mu(\tau'^2 + \Delta^2) - (\omega_0 + \omega_{d_2})\Delta - \omega_1\tau'$$

$$v = (\omega_1 - \omega_{d_2} - \mu\{\tau' - \Delta\})t + (\omega_0 + \omega_{d_2})\Delta + \frac{1}{2}\mu(\tau'^2 - \Delta^2) + \omega_1\tau'.$$

The limits of the integrals are determined by the envelope factors and the particular value of τ' .

These expressions can be significantly reduced by employing narrow-band assumptions. Integrals of the form

$$\int \cos(ax^2+2bx+c) dx = \sqrt{\frac{\pi}{2a}} \left\{ \cos\left(\frac{b^2-ac}{a}\right) C\left[\sqrt{\frac{2}{a\pi}}(ax+b)\right] + \sin\left(\frac{b^2-ac}{a}\right) S\left[\sqrt{\frac{2}{a\pi}}(ax+b)\right] \right\} \quad (2-12a)$$

and

$$\int \sin(ax^2+2bx+c) dx = \sqrt{\frac{\pi}{2a}} \left\{ \cos\left(\frac{b^2-ac}{a}\right) S\left[\sqrt{\frac{2}{a\pi}}(ax+b)\right] - \sin\left(\frac{b^2-ac}{a}\right) C\left[\sqrt{\frac{2}{a\pi}}(ax+b)\right] \right\} \quad (2-12b)$$

can be shown to be negligible under narrow-band considerations.

In these expressions, $C(z)$ and $S(z)$ are the Fresnel integrals

$$C(z) = \int_0^z \cos\left(\frac{\pi}{2}t^2\right) dt$$

$$S(z) = \int_0^z \sin\left(\frac{\pi}{2}t^2\right) dt.$$

Introduce the argument:

$$\theta = \frac{b^2-ac}{a} \quad (2-13)$$

If only the first reflection is considered, then

$$a = \mu$$

$$b = \frac{1}{2} (2\omega_o + \omega_i + \omega_{d_i} - \mu\tau')$$

$$c = \frac{1}{2} \mu\tau'^2 - \omega_i\tau'$$

For ω_i and $\omega_{d_i} \ll \omega_o$, Equation 2-13 reduces to

$$\theta = \frac{\omega_o^2 - \mu\omega_o\tau' - \frac{1}{4}\mu^2\tau'^2}{\mu} \quad (2-14)$$

If typical values of carrier frequency and rate of radian frequency sweep are substituted in Equation 2-14, it is not difficult to see that the expression is relatively independent of τ' . Hence, we may write

$$\theta \approx \frac{\omega_o^2}{\mu} .$$

The next item to be examined is the argument of the Fresnel integrals

$$\sqrt{\frac{2}{a\pi}}(ax+b) .$$

Again under narrow-band considerations, this expression can be written approximately as

$$\sqrt{\frac{2}{\mu\pi}}(\omega_o - \frac{\mu\tau'}{2}) .$$

Not only is this term relatively independent of τ' , but also the argument is a large number for representative values of carrier frequency and rate of radian frequency sweep. The values of both the sine and the cosine Fresnel integrals approach $\frac{1}{2}$ for large arguments. Consequently, the right hand member of Equations 2-12a and 2-12b can be written respectively as

$$\sqrt{\frac{\pi}{8a}}(\cos \theta + \sin \theta)$$

and

$$\sqrt{\frac{\pi}{8a}}(\cos \theta - \sin \theta) .$$

For $a = \mu$, these expressions contribute little to the integral in Equation 2-11. Therefore, terms having the form of Equations 2-12a and 2-12b can be neglected.

Hence, Equation 2-11 is written as

$$\psi(\tau', \omega, \Delta) = \left| \frac{\alpha_1}{T} \int_{\ell_1}^{\ell_2} e^{j[(\omega_1 - \omega_{d_1} - \mu\tau')t + \frac{1}{2} \mu\tau'^2 - \omega_1\tau']} dt \right. \\ \left. + \frac{\alpha_2}{T} \int_{\ell_3}^{\ell_4} e^{j[(\omega_1 - \omega_{d_2} - \mu(\tau' - \Delta))t + (\omega_0 + \omega_{d_2})\Delta + \frac{1}{2} \mu(\tau'^2 - \Delta^2) - \omega_1\tau']} dt \right|,$$

which can be reduced to

$$\psi(\tau', \omega, \Delta) = \left| \frac{\alpha_1}{T} \int_{\ell_1}^{\ell_2} e^{j[\omega_1 - \omega_{d_1} - \mu\tau']t} dt \right. \\ \left. + \frac{\alpha_2}{T} \int_{\ell_3}^{\ell_4} e^{j[(\omega_1 - \omega_{d_2} - \mu(\tau' - \Delta))t + (\omega_0 + \omega_{d_2})\Delta - \frac{1}{2} \mu\Delta^2]} dt \right|. \quad (2-15)$$

Equation 2-15 was coded in Fortran and programmed on an IBM 360 computer. By assuming a sequence of equispaced values for target doppler, a family of curves of ψ versus τ were computed for the zero doppler filter bank. The output was plotted by the computer in the form of an oblique projection as shown in Figure 2-3. The origin of the graph scale on the τ axis is set in relation to the particular curve at which doppler match occurs. In this figure, the middle curve represents doppler match between filter bank and target.

In order to affect comparison with the wideband ambiguity function derived and plotted in Chapter IV, sonar parameters were assumed. Consequently, the long pulse lengths common to sonar systems restrict the amount of pulse compression that can be assumed if the signal is to be considered narrow-band. (The requirements for a signal to be considered narrow-band are given in the next chapter.)

The parameters of Figure 2-3 are:

$$f_0 = 1000 \text{ Hz}$$

$$k = 10 \text{ Hz/sec}$$

$$T = 1 \text{ sec}$$

$$\Delta = .004 \text{ sec}$$

with equal echo amplitudes

$$\alpha_1 = \alpha_2 = 1.$$

Figure 2-4 is a plot of the same function for a delay of .01 seconds.

It is interesting to contrast Figure 2-3, the result of applying Equation 2-15 to a narrow-band signal, with the results obtained when a wideband signal is assumed and substituted in to this same narrow-band equation. Figure 2-5 is a plot for this wideband signal, which has the same parameters as the signal used in Figure 2-3 except that

$$k = 200 \text{ Hz/sec.}$$

In this graph, the delay Δ is distinctly observable. The echoes almost cancel, because of the wide bandwidth. Also noteworthy is the relative invariance of the doppler cuts of the ambiguity function over the complete range of target doppler.

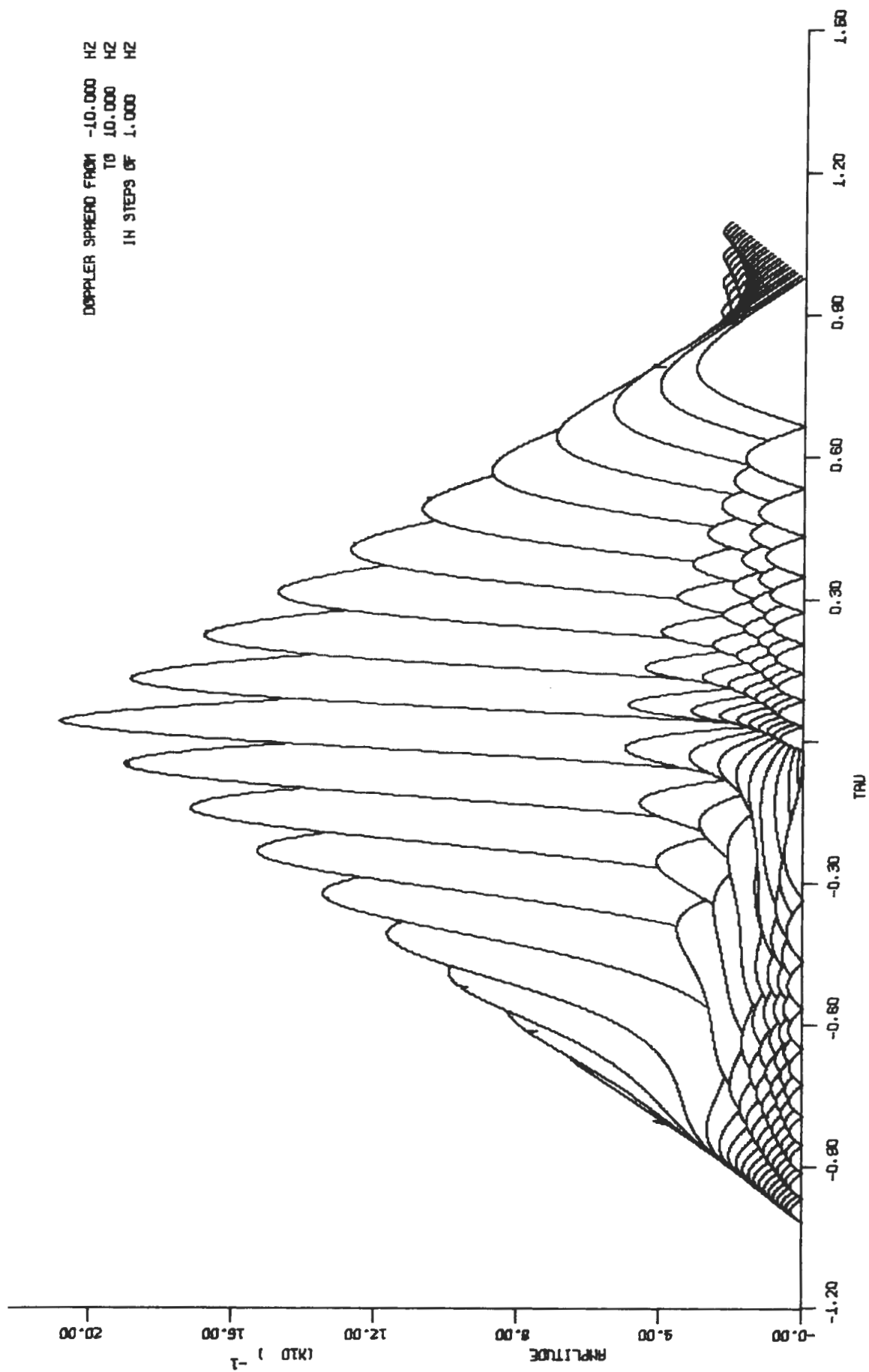


FIG. 2-3 NARROW-BAND GRAPH, DELAY = .004

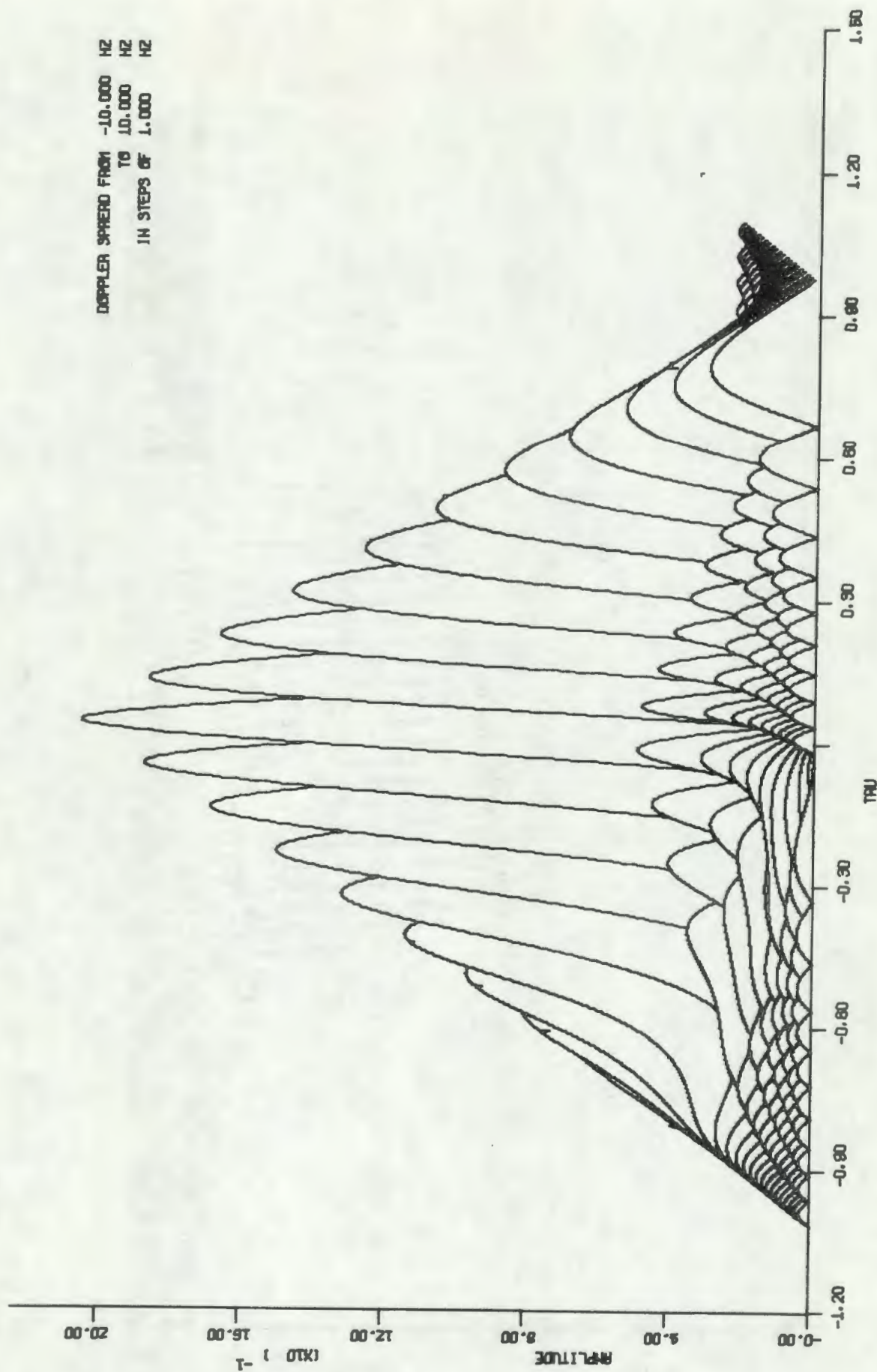


FIG. 2-4 NARROW-BAND GRAPH, DELAY = .010

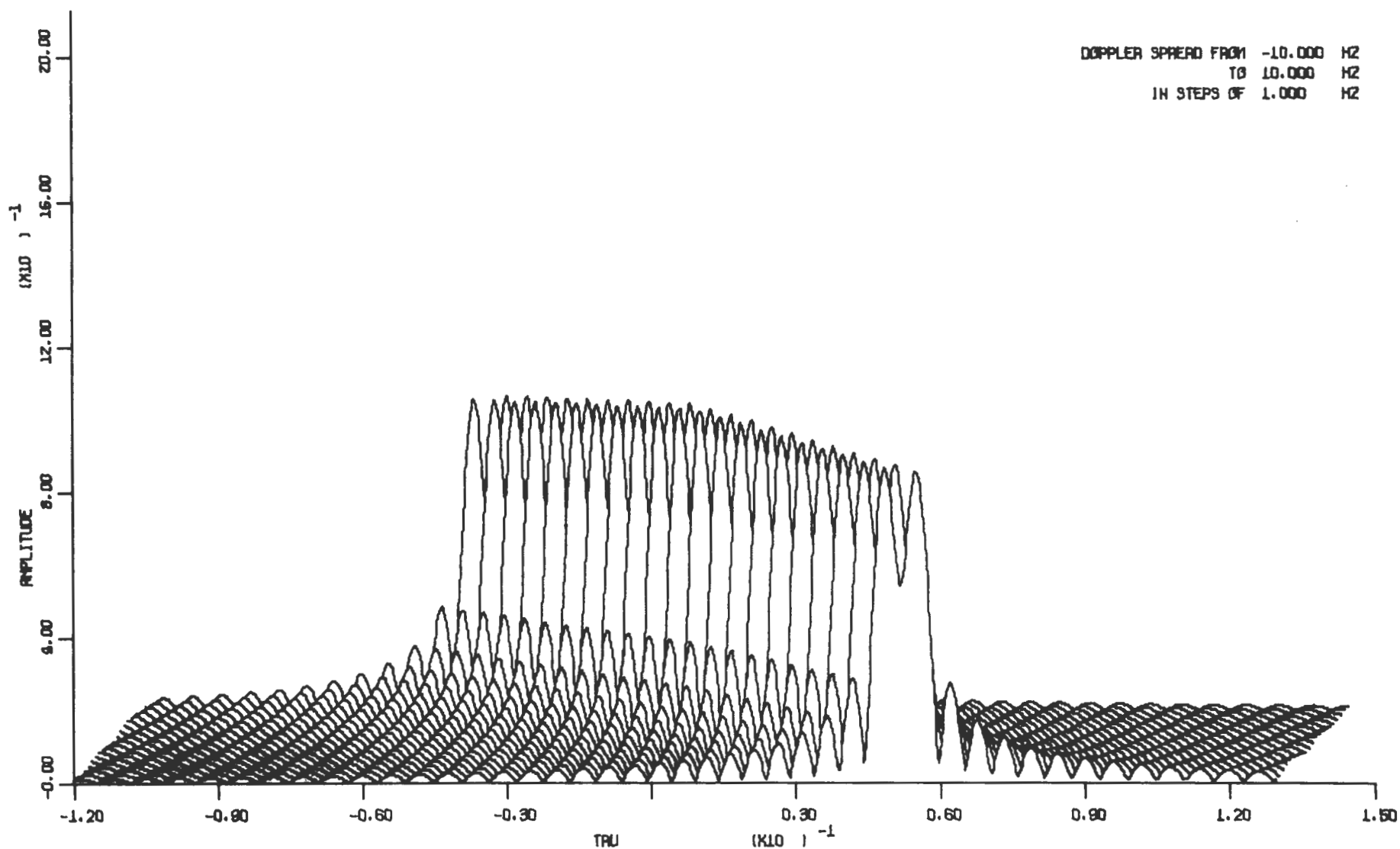


FIG. 2-5 NARROW-BAND GRAPH WITH WIDEBAND SIGNAL DELAY = .004

CHAPTER 3

WIDEBAND AMBIGUITY FUNCTION

A. BACKGROUND

As previously stated, the implications inherent in the use of the narrow-band ambiguity function are that the doppler effect does not significantly alter the envelope of the transmitted signal. This is a valid assumption in most radar cases. However, for sonar systems, the combination of lower carrier frequency, longer pulse length, and slower medium propagation speed makes this assumption restrictive.

The commonly accepted cross-over point between the narrow-band case and the wideband case occurs when⁶

$$v_r \ll \frac{c}{2TB}, \quad (3-1)$$

where

c = propagation speed in the medium

B = signal bandwidth

T = pulse width

v_r = radial velocity (assumed positive when the range is closing).

It has been shown that for the case of non-accelerating targets the inequality can be confined to⁷

$$v_r \lesssim \frac{1c}{BT}. \quad (3-2)$$

Taking representative sonar figures of

$B = 200 \text{ Hz}$

$T = 1 \text{ sec},$

we find that

$$v_r \lesssim 1.5 \text{ knots.}$$

It is obvious that narrow-band considerations do not apply.

Wideband ambiguity functions have been under investigation for some time. Perhaps the most noteworthy treatise on the subject is a paper by E. J. Kelly and R. R. Wishner,⁶ which presents a very detailed mathematical development of a wideband ambiguity function. References 8, 9, and 10 investigate the effects of an accelerating target on linear FM systems. Finally, References 11 and 12 expand the concept of a generalized ambiguity function.

S. A. Kramer utilized frequency versus time plots to examine the effect of wideband analysis on linear FM.⁹ His method offers the best insight into the problems associated with wideband systems. Therefore, the following section is a brief synopsis of Kramer's development.

In the narrow-band case, when there is a doppler mismatch, the received signal is simply shifted in frequency uniformly throughout its length some distance from the replica signal. The lines remain parallel because the pulse compression factor of the received signal is the same as that of the transmitted signal.

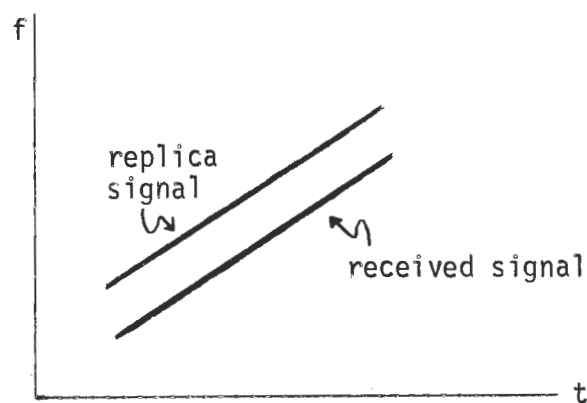


Fig. 3-1 Mismatched signals: Narrow-band case

In the wideband case, however, a slope change is introduced, caused by a pulse compression factor different from the pulse compression factor of the transmitted signal. Thus, if the replica signal does

not match the received signal in doppler, the two lines are not parallel.

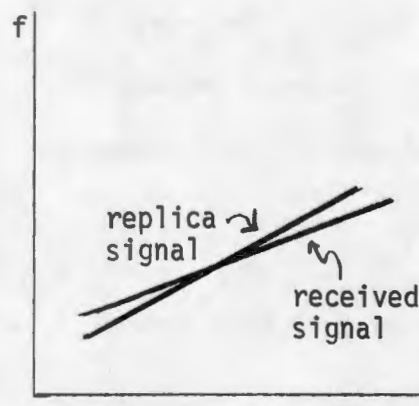


Fig. 3-2 Mismatched signals: Wideband case

Of course, if the received signal is exactly matched in doppler, then the two lines would be parallel even for the wideband case.

If the discussion is limited to targets of constant velocity, there are three effects of doppler on the returning signal:

1. The carrier frequency f_0 of the transmitted signal is shifted by the doppler frequency.
2. The envelope of the transmitted signal is altered.
3. The energy of the received signal differs from the transmitted signal energy.¹³

In the narrow-band case only the first effect is taken into consideration.

The following analysis reexamines the frequency shifting effect and introduces the other two considerations into the development of a wideband ambiguity function.

Each frequency component of the received signal can be written as

$$f_r = \left(\frac{1 + \frac{v_r}{c}}{1 - \frac{v_r}{c}} \right) f_t, \quad (3-3)$$

where

f_r = received frequency component

f_t = transmitted frequency component.

For $v_r \ll c$, Equation 3-3 can be approximated as

$$f_r \approx \left(1 + \frac{2v_r}{c}\right) f_t. \quad (3-4)$$

It is convenient to define a doppler factor, D , where

$$D = 1 + \frac{2v_r}{c}.$$

The doppler frequency, f_d , can be defined as the change in the initial frequency of the transmitted signal, f_{ot} , or

$$f_d = f_{or} - f_{ot}.$$

But, from Equation 3-4,

$$f_{or} = D f_{ot},$$

$$f_d = (D-1) f_{ot},$$

and

$$D = 1 + \frac{f_d}{f_o}, \quad (3-5)$$

which shows the relationship between the doppler factor and the doppler frequency.

The transmitted signal can be written in the frequency domain by taking the Fourier Transform of $s(t)$,

$$S(f) = F[s(t)].$$

The received signal can be expressed in terms of the transmitted signal in the frequency domain as

$$R(f) = S\left(\frac{f}{D}\right).$$

Now the received signal can be written as the inverse Fourier transform of $S(\frac{f}{D})$,

$$r(t) = F^{-1}[S(\frac{f}{D})] = \int_{-\infty}^{\infty} S(\frac{f}{D}) e^{j2\pi ft} df. \quad (3-6)$$

Introducing a change of variable, $f' = \frac{f}{D}$, Equation 3-6 becomes

$$r(t) = D \int_{-\infty}^{\infty} S(f') e^{j2\pi f' (Dt)} df'. \quad (3-7)$$

This is the normal inverse Fourier transform, except that the transformation is into the revised time domain Dt . Equation 3-7 becomes

$$r(t) = Ds(Dt),$$

which for a linear FM signal is written

$$r(t) = ADX(Dt) \cos \{ \omega_0 Dt + \frac{1}{2} \mu (Dt)^2 \}. \quad (3-8)$$

If Equation 3-8 is now examined, it can be seen that the three effects of wideband analysis have occurred.

1. The frequency components of the transmitted signal are shifted by the doppler frequency. For, the instantaneous frequency of the received signal can be written as

$$\omega_0 D + \mu D^2 t.$$

But from Equation 4-5 this can be written

$$\begin{aligned} & \omega_0 \left(1 + \frac{f_d}{f_0} \right) + \mu D^2 t \\ &= \omega_0 + \omega_d + \mu D^2 t \end{aligned}$$

Thus, not only has the initial frequency been shifted but effectively there is a new pulse compression factor $\mu D^2 T$. This accounts for the difference in slopes of Figure 3-2.

2. The envelope of the transmitted signal is altered. This has occurred through the new definition of the envelope term $X(Dt)$.

For

$$\begin{aligned} X(Dt) &= u(Dt) - u(Dt - T) \\ &= u(D\{t\}) - u(D\{t - \frac{T}{D}\}) \\ &= u(t) - u(t - \frac{T}{D}) . \end{aligned}$$

From this expression, the expansion or compression of the pulse is shown to be dependent on the value of the doppler factor D.

3. Finally, the energy of the return signal has been changed by the doppler factor D. Reference 13 showed that the ratio of the received signal energy density to the transmitted signal energy density is given by D.

The energy of the signal of Equation 3-8

$$\begin{aligned} &= \int_{-\infty}^{\infty} A^2 D^2 X(Dt) X(Dt) \cos^2(\omega_0 Dt + \frac{1}{2} \mu D^2 t^2) dt \\ &= \int_0^{T/D} A^2 D^2 \cos^2(\omega_0 Dt + \frac{1}{2} \mu D^2 t^2) dt \\ &= \frac{A^2 D^2 t}{2} \Big|_0^{T/D} \\ &= D . \end{aligned}$$

B. GENERAL DEVELOPMENT OF THE WIDEBAND AMBIGUITY FUNCTION FOR ECHO SPLITTING

The output of a matched filter is written as

$$\Lambda = \int_{-\infty}^{\infty} r(t) s^* \omega_i(t-\tau) dt, \quad (3-9)$$

which will be recognized from the narrow-band discussion.

Investigation of Equation 3-9 might be accomplished by writing the received and replica signals in canonic form as:

$$r(t) = \text{Re}[R(t)e^{j\omega_0 t}] \quad (3-10a)$$

$$s'_{\omega_1}(t-\tau) = \text{Re}[S'_{\omega_1}(t-\tau)e^{j\omega_0(t-\tau)}], \quad (3-10b)$$

where as before,

$$R(t) = \text{DAX}(Dt)e^{j(\omega_d t + \frac{1}{2} \mu D^2 t^2)}$$

and

$$S'_{\omega_1}(t) = X(Dt) \left| S'_o(t) \right| e^{j(\omega_1 t + \frac{1}{2} \mu D^2 t^2)}.$$

Recalling that $\text{Re}[z(t)]$ can be written as

$$\frac{1}{2}[z(t) + z^*(t)],$$

Equation 3-9 can be written as

$$\begin{aligned} \Lambda = \frac{1}{4} \int_{-\infty}^{\infty} [R(t)e^{j\omega_0 t} S'_{\omega_1}(t-\tau)e^{j\omega_0(t-\tau)} + R(t)e^{j\omega_0 t} S'^*_{\omega_1}(t-\tau)e^{-j\omega_0(t-\tau)} \\ + R^*(t)e^{-j\omega_0 t} S'_{\omega_1}(t-\tau)e^{j\omega_0(t-\tau)} + R^*(t)e^{-j\omega_0 t} S'^*_{\omega_1}(t-\tau)e^{-j\omega_0(t-\tau)}] dt. \end{aligned} \quad (3-11)$$

If the terms, $R(t)e^{j\omega_0 t}$ and $S'_{\omega_1}(t-\tau)e^{j\omega_0(t-\tau)}$ are analytic, then since it is possible to state that the correlation integral of two analytical signals or the correlation integral of the complex conjugates of two analytical signals is zero, Equation 3-11 reduces to¹¹

$$\Lambda = \frac{1}{2} \int_{-\infty}^{\infty} R(t) S'^*_{\omega_1}(t-\tau)e^{j\omega_0 \tau} dt. \quad (3-12)$$

As this is the output of a matched filter, the ambiguity function can be arrived at by simply taking the envelope of Equation 3-12. If such an envelope could realistically be formed (in the wideband case, this is not a moot question),^{11,13} the ambiguity function would be written as

$$\psi(\tau, \omega) = \left| \frac{1}{2} \int_{-\infty}^{\infty} R(t) S'^*_{\omega_1}(t-\tau) dt \right|. \quad (3-13)$$

The fine structure, attributable to the carrier phase term $e^{j\omega_o\tau}$, has been omitted by the process of taking the absolute value. It is the same function as developed by Siebert in the narrow-band case. For narrow-band analysis, this thesis rejected Siebert's definition of the ambiguity function in the echo-splitting environment, because of the absence of the carrier frequency term. In addition, the assumption that an analytic signal model is appropriate under wideband conditions is highly suspect.

Consequently, the only recourse is to accept Equation 3-9 as the output of the matched filter and begin at that point to devise a suitable ambiguity function. As it is the envelope of this expression that is being used for the definition of the ambiguity function, the fine structure is removed simply by taking the absolute value of Equation 3-9. The ambiguity function is then written

$$\psi(\tau, \omega) = \left| \int_{-\infty}^{\infty} r(t) S'_{\omega_i}(t-\tau) e^{j\omega_o t} dt \right| \quad (3-14)$$

which is the same form as that used in Chapter II for the narrow-band case.

CHAPTER 4

WIDEBAND AMBIGUITY FUNCTION FOR DOUBLE-ECHO CASE

A. SYSTEM MODEL

If the time origin is taken as the starting point of the transmitted signal, then Equation 3-8 may be written as

$$r(t) = ADX(D\{t-t_d\}) \cos\{\omega_0 D(t-t_d) + \frac{1}{2} \mu D^2(t-t_d)^2\}.$$

The system model for generating a wideband ambiguity function might be constructed to be similar to Figure 2-1. Figure 4-1 and Figure 4-2 are possible models for the wideband analysis.

The output of the matched filter for the k^{th} range estimate τ_k , and the i^{th} doppler filter, is written

$$y(\tau_k, \omega_i) = \frac{2}{T} \int_{-\infty}^{\infty} DX(D\{t-t_d\}) \cos\{\omega_0 D(t-t_d) + \frac{1}{2} \mu D^2(t-t_d)^2\} \\ \cdot X(D_1 t - \tau_k) \cos\{\omega_0 (D_1 t - \tau_k) + \frac{1}{2} \mu (D_1 t - \tau_k)^2\} dt. \quad (4-1)$$

Defining

$$t' = t - t_d$$

and

$$D_1 \tau' = \tau_k - D_1 t_d,$$

Equation 4-1 is written as

$$y(\tau', \omega_i) = \frac{2}{T} \int_{-\infty}^{\infty} DX(Dt') \cos\{\omega_0 Dt' + \frac{1}{2} \mu (Dt')^2\} X\{D_1(t' - \tau')\} \\ \cdot \cos\{\omega_0 (D_1[t' - \tau']) + \frac{1}{2} \mu (D_1[t' - \tau'])^2\} dt'. \quad (4-2)$$

This can now be referred to the time base of the replica signal by defining

$$D_1 t' = t^*$$

and

$$\frac{D}{D_1} = D'.$$

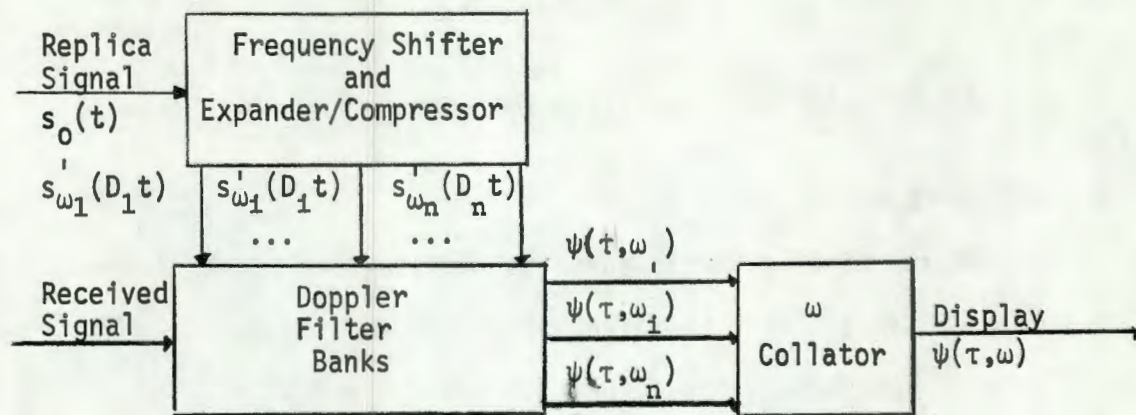


Fig. 4-1 ENVELOPE OF THE OUTPUT OF A MATCHED FILTER

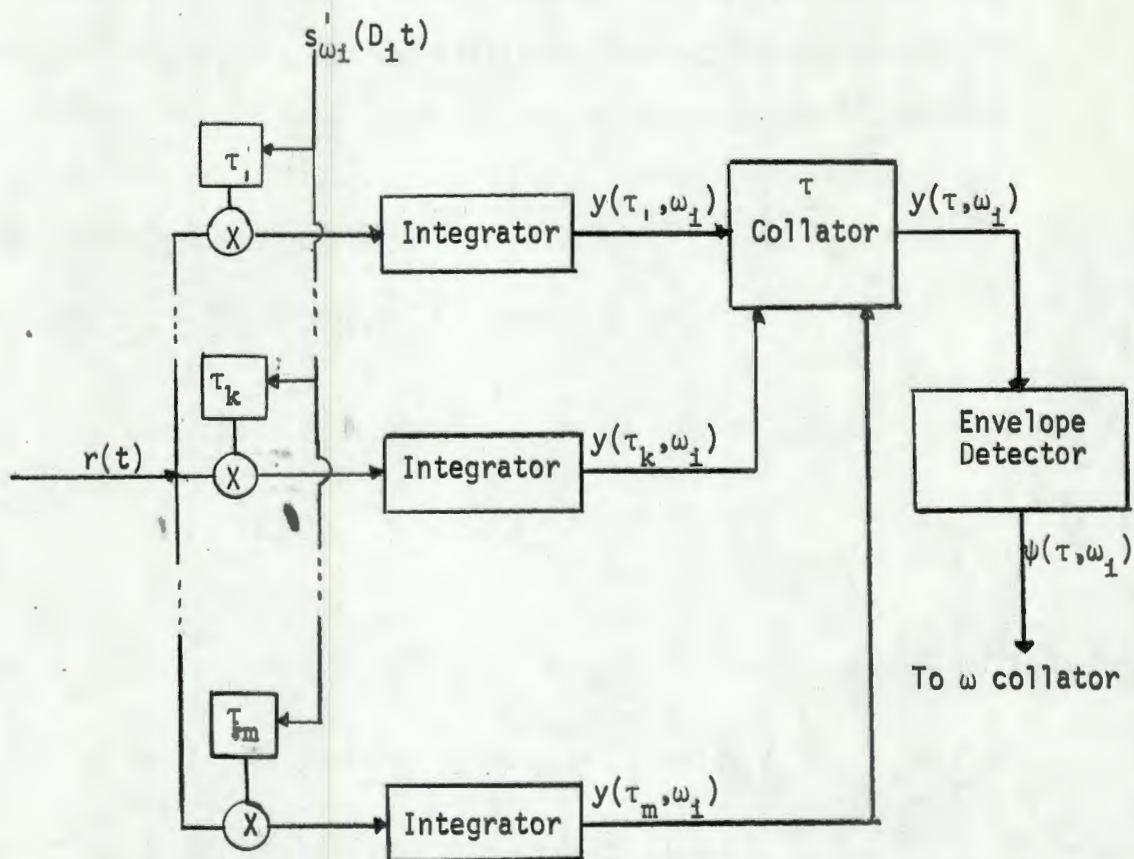


Fig. 4-2 i^{th} DOPPLER FILTER

With these substitutions, Equation 4-2 can be written as

$$y(\tau', \omega_i) = \frac{2}{T} \int_{-\infty}^{\infty} D' X(D' t^*) \cos\{\omega_o D' t^* + \frac{1}{2}\mu(D' t^*)^2\} X(t^* - D_i \tau') \cdot \cos\{\omega_o (t^* - D_i \tau') + \frac{1}{2}\mu(t^* - D_i \tau')^2\} dt^*. \quad (4-3)$$

From the substitutions that have been made, it is seen that when

$$D_i \tau' = 0,$$

$$\tau_k = D_i t_d.$$

Thus, if the system of Figure 4-1 is used, the doppler factor enters into the determination of range.

If, on the other hand, another model for the system is chosen, this problem does not arise. Figure 4-3 and Figure 4-4 describe such a system. For, with this as the model, the output of the matched filter for the k^{th} range gate and the i^{th} doppler filter is written as

$$y(\tau_k, \omega_i) = \frac{2}{T} \int_{-\infty}^{\infty} DX(D[t-t_d]) \cos\{\omega_o D(t-t_d) + \frac{1}{2}\mu(D[t-t_d])^2\} \cdot X(D_i[t-\tau_k]) \cos\{\omega_o D_i(t-\tau_k) + \frac{1}{2}\mu(D_i[t-\tau_k])^2\} dt. \quad (4-4)$$

Now if we define

$$t' = t - t_d$$

and

$$\tau' = \tau_k - t_d,$$

Equation 4-4 becomes

$$y(\tau', \omega_i) = \frac{2}{T} \int_{-\infty}^{\infty} DX(Dt') \cos\{\omega_o Dt' + \frac{1}{2}\mu(Dt')^2\} X(D_i[t'-\tau']) \cdot \cos\{\omega_o D_i(t'-\tau') + \frac{1}{2}\mu(D_i[t'-\tau'])^2\} dt'. \quad (4-5)$$

As in the preceding example, this expression is now referred to the time frame of the replica signal and is written as

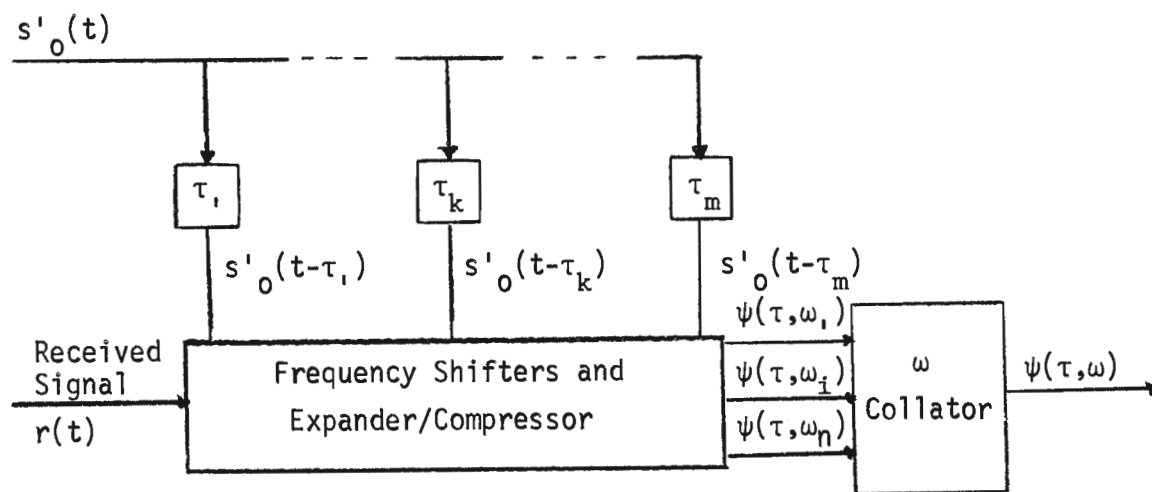


Fig. 4-3 ENVELOPE OF MATCHED FILTER OUTPUT

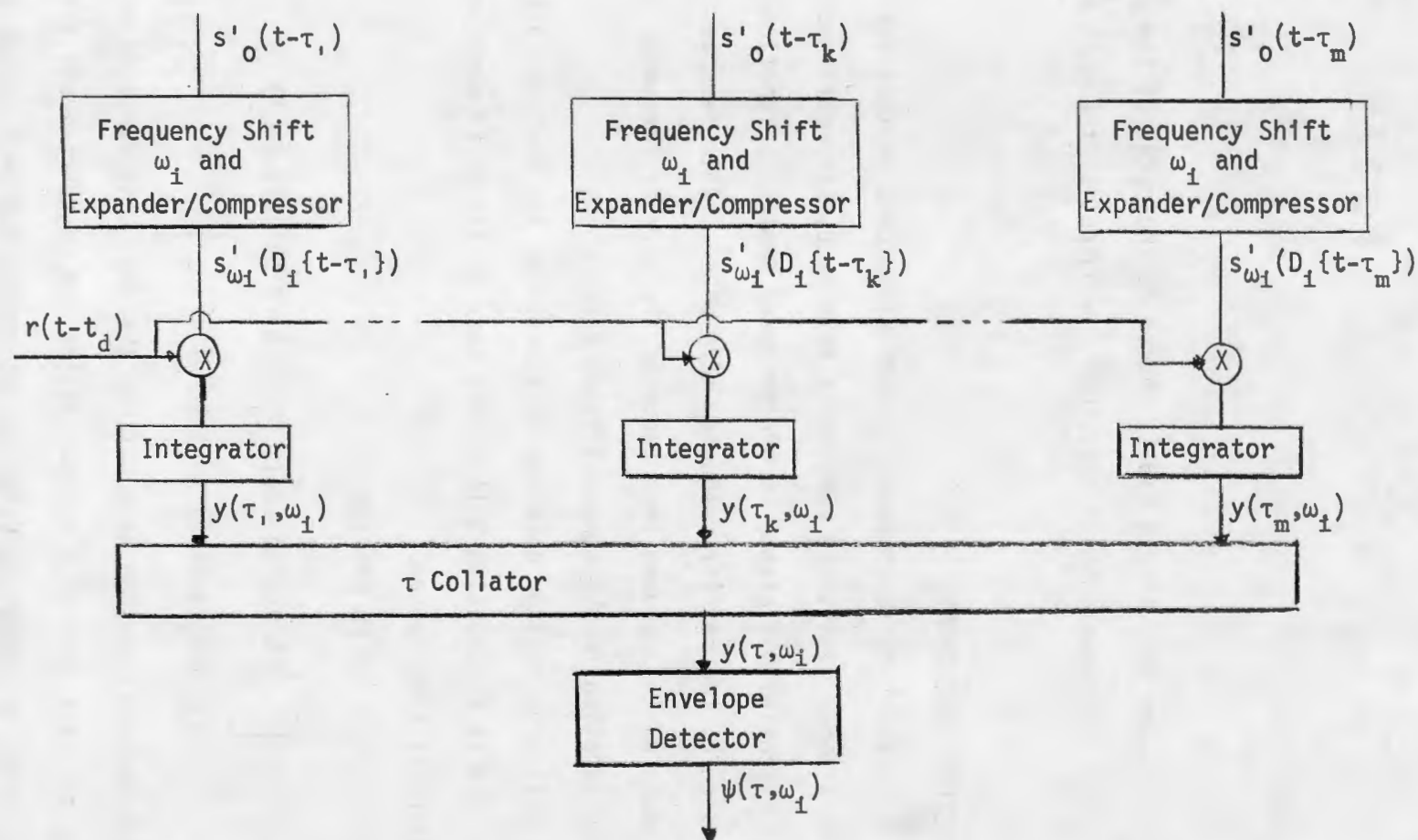


Fig. 4-4 i^{th} DOPPLER BANK

$$y(\tau', \omega_1) = \frac{2}{T} \int_{-\infty}^{\infty} D' X(D' t^*) \cos\{\omega_0 D' t^* + \frac{1}{2}\mu(D' t^*)^2\} X(t^* - D_1 \tau') \cdot \cos\{\omega_0(t^* - D_1 \tau') + \frac{1}{2}\mu(t^* - D_1 \tau')^2\} dt^*. \quad (4-6)$$

Now when

$$D_1 \tau' = 0,$$

it is seen that

$$\tau_k = t_d.$$

It is for this reason that Figure 4-3 is chosen as the model of the system. Accordingly, Equation 4-4 describes the output of the matched filter.

B. SINGLE-RETURN DEVELOPMENT

It is interesting to compare the ambiguity function that was derived in this paper with those previously developed. As mentioned earlier, the essential difference in our proposed ambiguity function is the inclusion of the carrier frequency term $e^{j\omega_0 t}$. This term was included because of the assumed importance of the carrier frequency on the ambiguity function in the echo-splitting case.

The following section develops an expression for the ambiguity function arrived at in Equation 3-14 in the case of linear FM when only a single return is experienced.

Equation 4-6 can be written as

$$y(\tau', \omega_1) = \text{Re} \left[\frac{2}{T} \int_{-\infty}^{\infty} D' X(D' t) \cos\{\omega_0 D' t + \frac{1}{2}\mu(D' t)^2\} X(t - D_1 \tau') \cdot e^{j[\omega_0(t - D_1 \tau') + \frac{1}{2}\mu(t - D_1 \tau')^2]} dt \right]. \quad (4-7)$$

As in the narrow-band case, we have defined the ambiguity function as the envelope of the output of a matched filter and we approximate this envelope by taking the absolute value of the expression in Equation 4-7.

The final result for the linear FM case with single return is

$$\psi(\tau', \omega_1) = \left| \frac{2}{T} \int_{-\infty}^{\infty} D' X(D't) \cos\{\omega_0 D't + \frac{1}{2}\mu(D't)^2\} X(t-D_1\tau') \cdot e^{j[\omega_0 t + \frac{1}{2}\mu(t-D_1\tau')^2]} dt \right|. \quad (4-8)$$

Computer outputs of this function utilizing various sonar parameters are shown in Figures 4-5 through 4-7. One interesting property of this function is the apparent splitting of the pulse for the non-matched condition. It is also interesting to note the narrow doppler tolerance of this function. This is true of all wideband functions.⁹

C. DOUBLE-ECHO EXAMPLE

If the echo-splitting case is now considered, the received signal, $r(t)$, is written as

$$r(t) = \sum_{j=1}^N A\alpha_j D_j X(D_j[t-t_{d_j}]) \cos\{\omega_0 D_j(t-t_{d_j}) + \frac{1}{2}\mu(D_j[t-t_{d_j}])^2\}. \quad (4-9)$$

Assuming once again that there are only two reflectors, Equation 4-9 becomes

$$r(t) = A\alpha_1 D_1 X(D_1[t-t_{d_1}]) \cos\{\omega_0 D_1(t-t_{d_1}) + \frac{1}{2}\mu(D_1[t-t_{d_1}])^2\} + A\alpha_2 D_2 X(D_2[t-t_{d_2}]) \cos\{\omega_0 D_2(t-t_{d_2}) + \frac{1}{2}\mu(D_2[t-t_{d_2}])^2\}.$$

$y(\tau, \omega_1)$ is then written as

$$y(\tau, \omega_1) = \text{Re} \left\langle \frac{2}{T} \int_{-\infty}^{\infty} \left[\alpha_1 D_1 X(D_1[t-t_{d_1}]) \cos\{\omega_0 D_1(t-t_{d_1}) + \frac{1}{2}\mu(D_1[t-t_{d_1}])^2\} + \alpha_2 D_2 X(D_2[t-t_{d_2}]) \cos\{\omega_0 D_2(t-t_{d_2}) + \frac{1}{2}\mu(D_2[t-t_{d_2}])^2\} \right] \cdot X(D_1[t-\tau]) e^{j[\omega_0 D_1(t-\tau) + \frac{1}{2}\mu(D_1[t-\tau])^2]} dt \right\rangle. \quad (4-10)$$

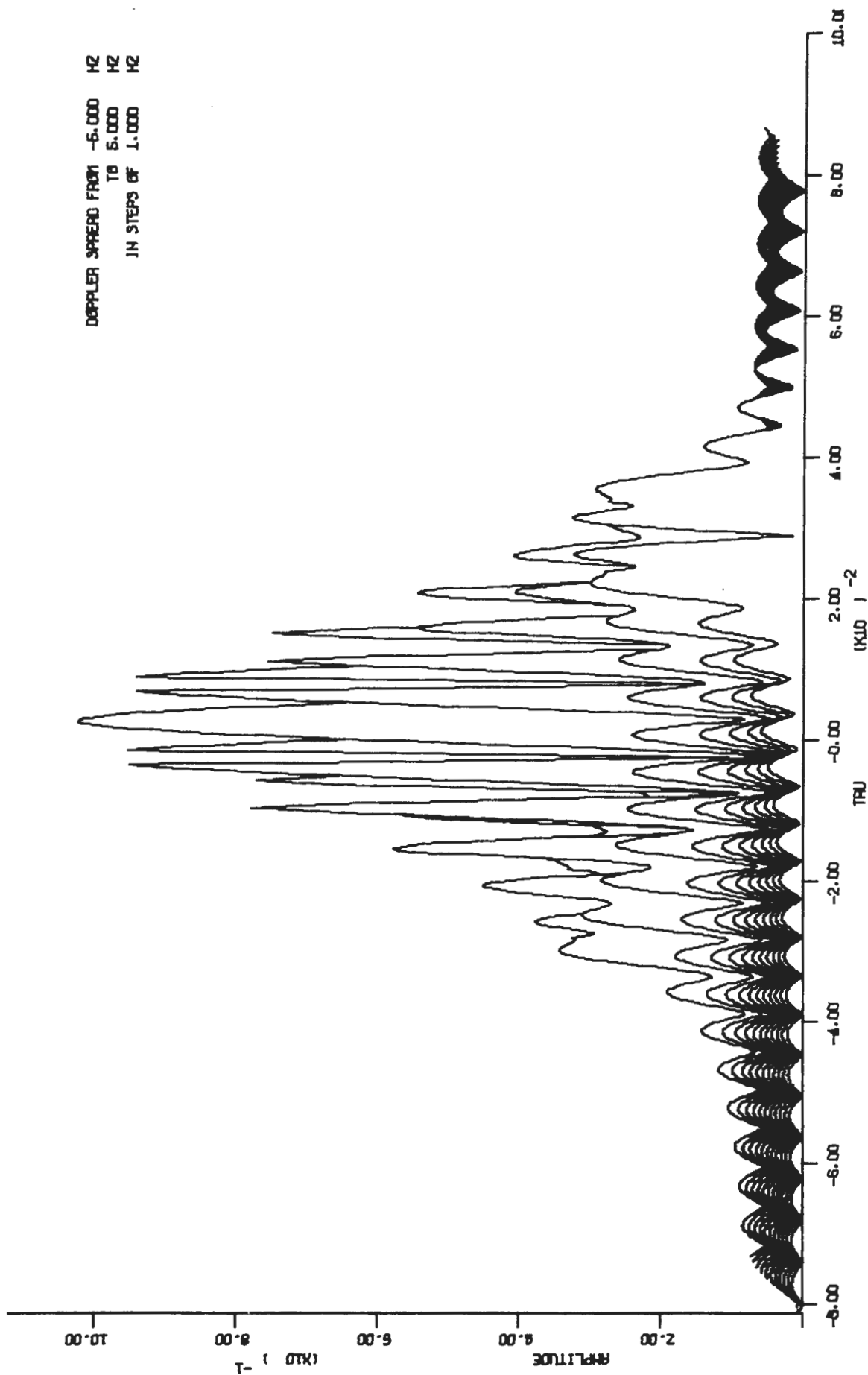


FIG. 4-5 SINGLE-RETURN WIDEBAND AMBIGUITY FUNCTION

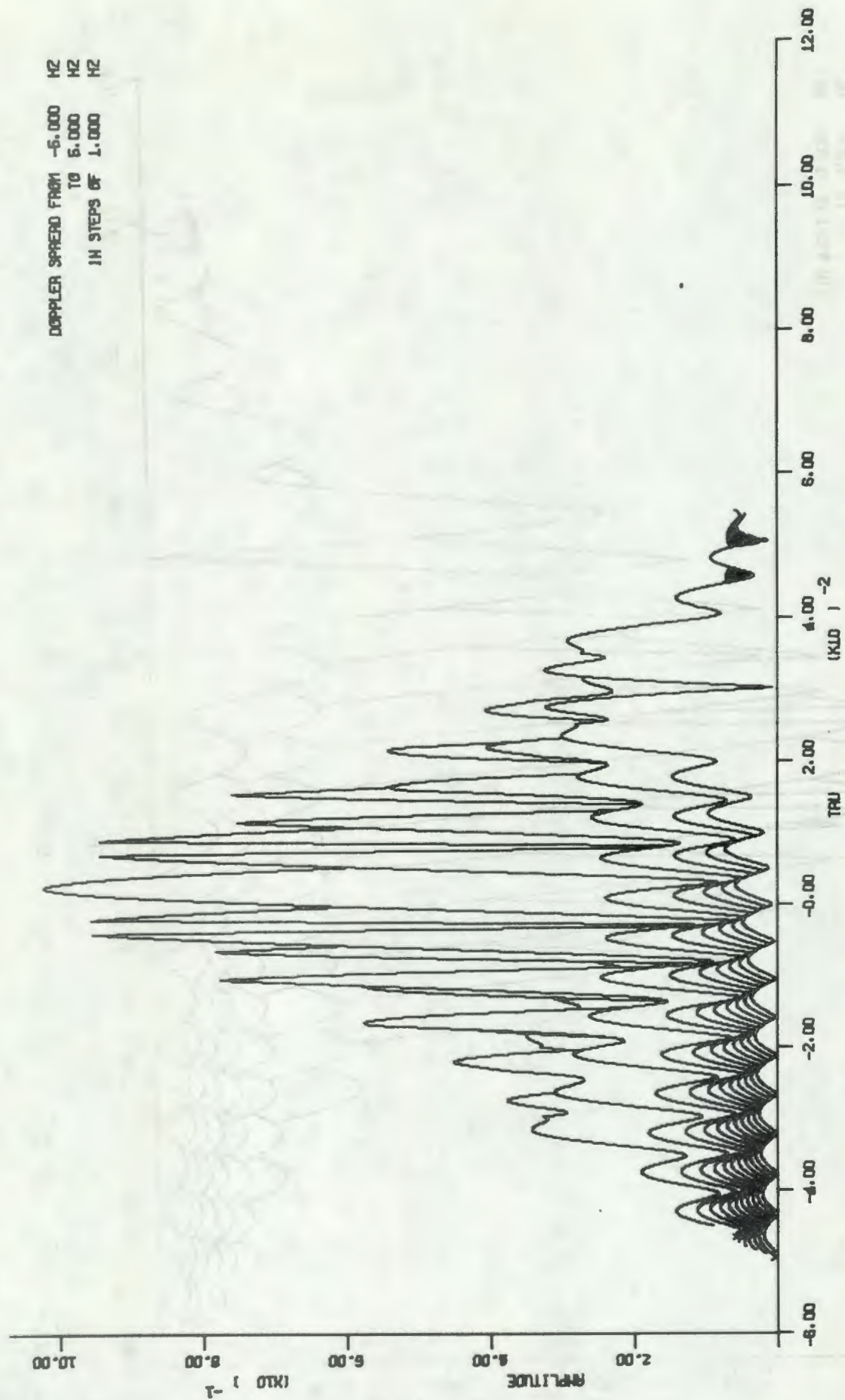


FIG. 4-6 SINGLE-RETURN WIDEBAND AMBIGUITY FUNCTION

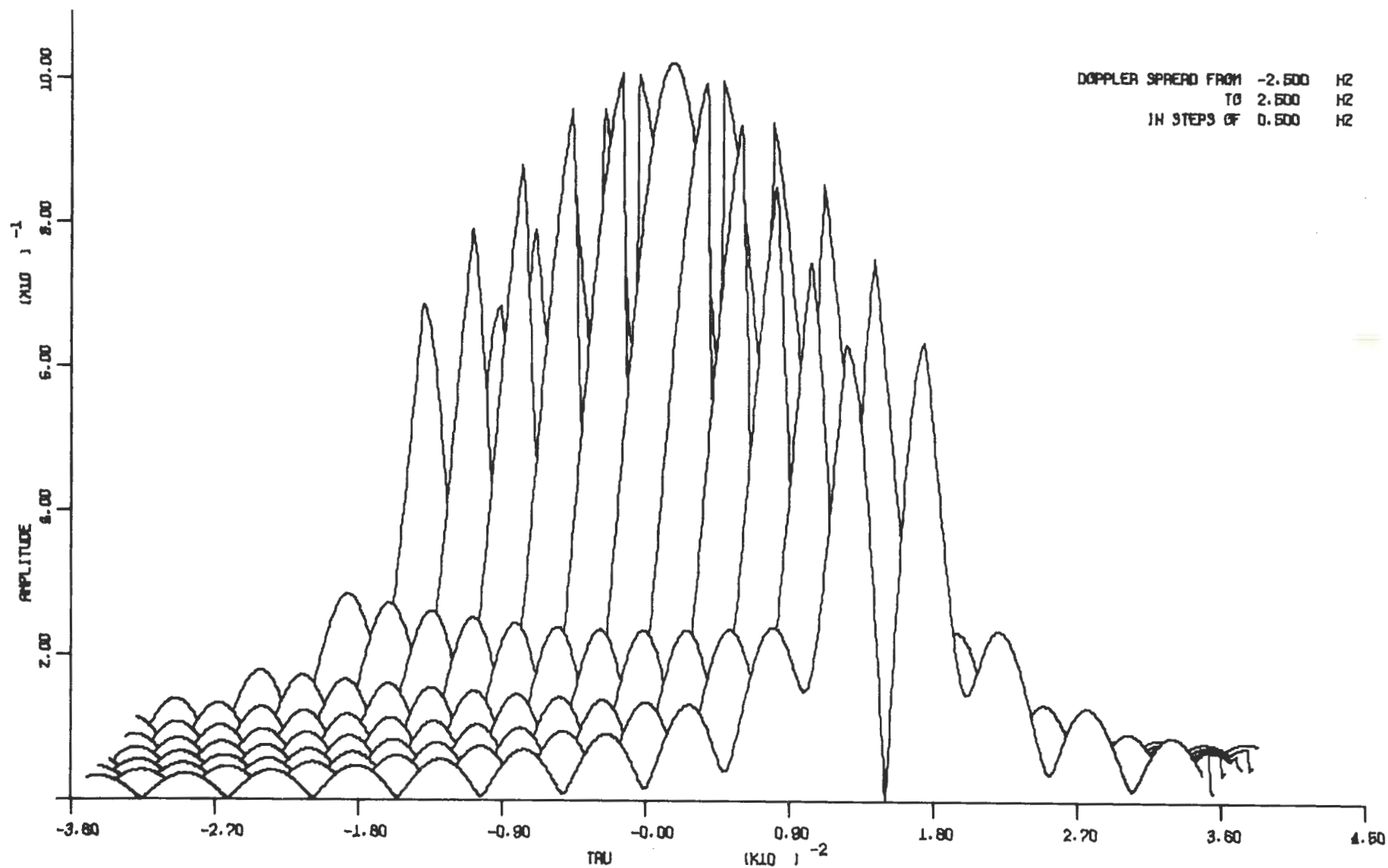


FIG. 4-7 SINGLE-RETURN WIDEBAND AMBIGUITY FUNCTION

If the envelope of this expression is now taken, Equation 4-10 is written

$$\begin{aligned} \psi(\tau, \omega_1) = \frac{2}{T} \left| \int_{-\infty}^{\infty} \left[\alpha_1 D_1 X(D_1[t-t_{d1}]) \cos\{\omega_0 D_1(t-t_{d1}) + \frac{1}{2}\mu(D_1[t-t_{d1}])^2\} \right. \right. \\ \left. \left. + \alpha_2 D_2 X(D_2[t-t_{d2}]) \cos\{\omega_0 D_2(t-t_{d2}) + \frac{1}{2}\mu(D_2[t-t_{d2}])^2\} \right] \right. \\ \left. \cdot X(D_1[t-\tau]) e^{j\{\omega_0 D_1(t-\tau) + \frac{1}{2}\mu(D_1[t-\tau])^2\}} dt \right| . \end{aligned} \quad (4-11)$$

By defining

$$t' = t - t_{d1},$$

$$\Delta = t_{d2} - t_{d1},$$

and

$$\tau' = \tau - t_{d1},$$

Equation 4-11 becomes

$$\begin{aligned} \psi(\tau', \omega_1, \Delta) = \frac{2}{T} \left| \int_{-\infty}^{\infty} \left[\alpha_1 D_1 X(D_1 t') \cos\{\omega_0 D_1 t' + \frac{1}{2}\mu(D_1 t')^2\} + \alpha_2 D_2 X(D_2[t' - \Delta]) \right. \right. \\ \left. \left. \cdot \cos\{\omega_0 D_2(t' - \Delta) + \frac{1}{2}\mu(D_2[t' - \Delta])^2\} \right] \right. \\ \left. \cdot X(D_1[t' - \tau']) e^{j\{\omega_0 D_1(t' - \tau') + \frac{1}{2}\mu(D_1[t' - \tau'])^2\}} dt' \right| . \end{aligned} \quad (4-12)$$

Finally, by defining the quantities

$$D' = \frac{D_1}{D_1}$$

$$D'' = \frac{D_2}{D_1}$$

and referencing all returns to the replica signal by the transformation

$$D_1 t' = t^* = t ,$$

Equation 4-12 can be expressed as

$$\begin{aligned} \psi(\tau', \omega_1, \Delta) = \frac{2}{T} \left| \int_{-\infty}^{\infty} \left[\alpha_1 D' X(D't) \cos\{\omega_0 D't + \frac{1}{2}\mu(D't)^2\} + \alpha_2 D'' X(D''[t-D_1\Delta]) \right. \right. \\ \left. \cdot \cos\{\omega_0 D''(t-D_1\Delta) + \frac{1}{2}\mu(D''[t-D_1\Delta])^2\} \right] \\ \left. \cdot X(t-D_1\tau') e^{j[\omega_0 t + \frac{1}{2}\mu(t-D_1\tau')^2]} dt \right| . \end{aligned} \quad (4-13)$$

As a final substitution we define

$$D_1\tau' = \tau'' .$$

The final expression for the ambiguity function of the linear FM system is

$$\begin{aligned} \psi(\tau'', \omega_1, \Delta) = \frac{2}{T} \left| \int_{-\infty}^{\infty} \left[\alpha_1 D' X(D't) \cos\{\omega_0 D't + \frac{1}{2}\mu(D't)^2\} \right. \right. \\ \left. + \alpha_2 D'' X(D''[t-D_1\Delta]) \cos\{\omega_0 D''(t-D_1\Delta) + \frac{1}{2}\mu(D''[t-D_1\Delta])^2\} \right] \\ \left. \cdot X(t-\tau'') e^{j[\omega_0 t + \frac{1}{2}\mu(t-\tau'')^2]} dt \right| . \end{aligned} \quad (4-14)$$

It is important to note a fundamental difference between the ambiguity function above and that developed in the narrow-band case.

In the narrow-band case two paths are open for further investigation:

1. Plots of different replica signals can be correlated with a target of particular range and doppler.
2. Plots of a particular replica signal can be correlated with targets of various velocities.

In the wideband case, the fact that our function is plotted versus τ'' , which by definition is proportional to D_1 , restricts the choice to Case 2, if meaningful results are to be obtained.

It can be shown that with suitable approximations, Equation 4-14 reduces to Equation 2-10 developed in the narrow-band case. Appendix B develops the various equations needed to evaluate Equation 4-14.

Figures 4-8 and 4-9 are sample plots of Equation 4-14 for the 0 doppler bank. The plotting procedure is the same as that used in the narrow-band analysis. Basic parameters for these plots are:

$$f_0 = 1000 \text{ Hz}$$

$$k = 200 \text{ Hz/sec}$$

$$T = 1 \text{ sec}$$

and

$$\alpha_1 = \alpha_2 = 1.$$

For Figure 4-8, a delay of .003 seconds is assumed and for Figure 4-9, a delay of .004. No significant difference exists between these two families of curves.

Figure 4-7 may be compared with Figures 4-8 and 4-9. Since Figure 4-7 represents results for a single echo, $\alpha_1 = 1$ and $\alpha_2 = 0$, one must mentally double its ordinates before comparison. Furthermore, the doppler intervals between curves are 2.5 times greater. With these qualifications, the figures show that for $\Delta = .003$ and .004, the amplitude of the ambiguity function is less than for $\Delta = 0$, and the peak is somewhat broadened. With a time-bandwidth product TB of 200, the main peak for the zero doppler cut of the single-echo ambiguity function should have first nulls at $\tau = \pm \frac{T}{TB} = \pm .005 \text{ sec}$. The limiting value of Δ for double-echo resolution is thus approximately 5 milliseconds. For $\Delta = 10$ milliseconds, a complete echo split should occur.

Time limitations, as required for computer plotting, precluded generating further echo-splitting exhibits at this time.

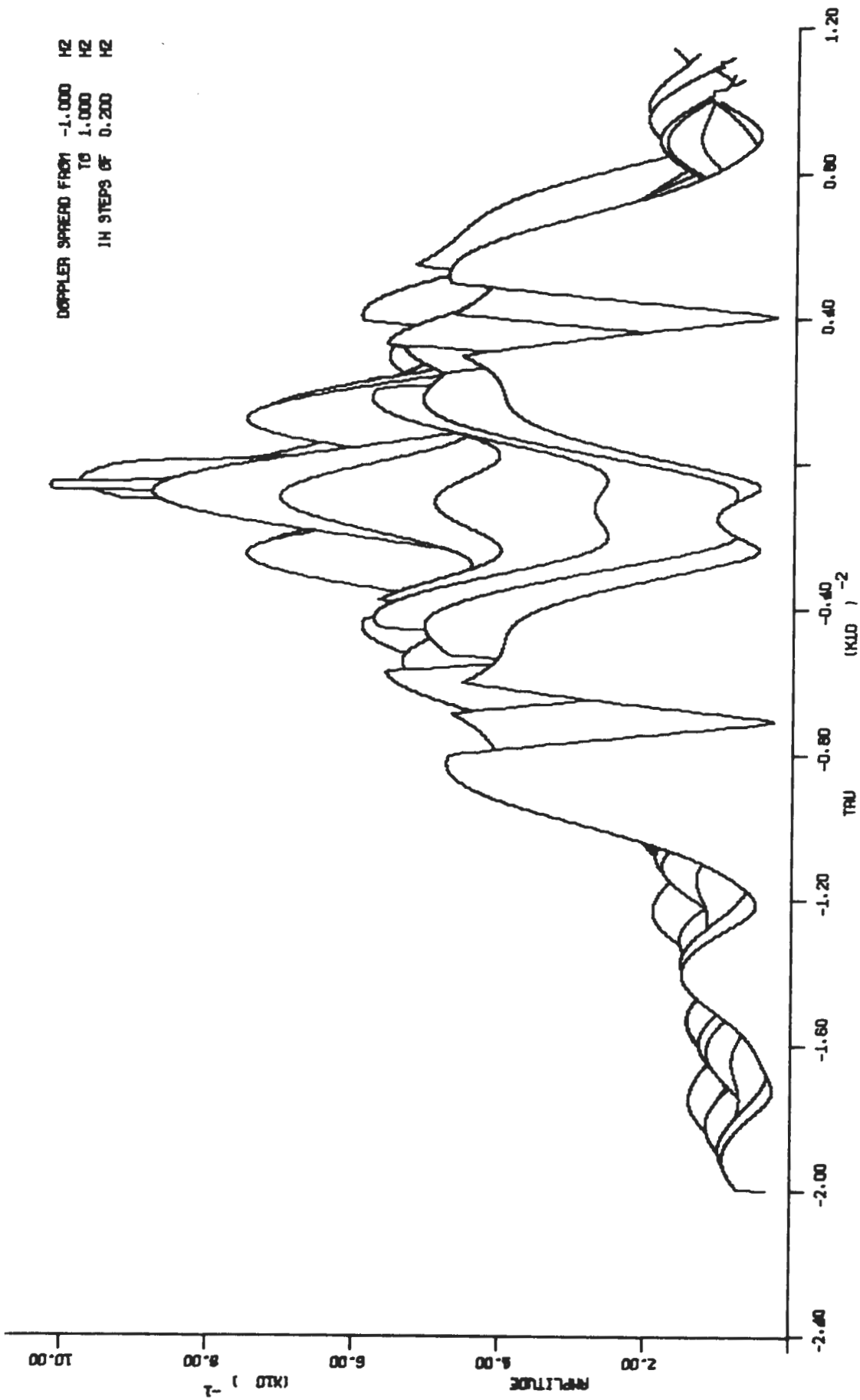


FIG. 4-8 WIDEBAND GRAPH, DELAY=.003

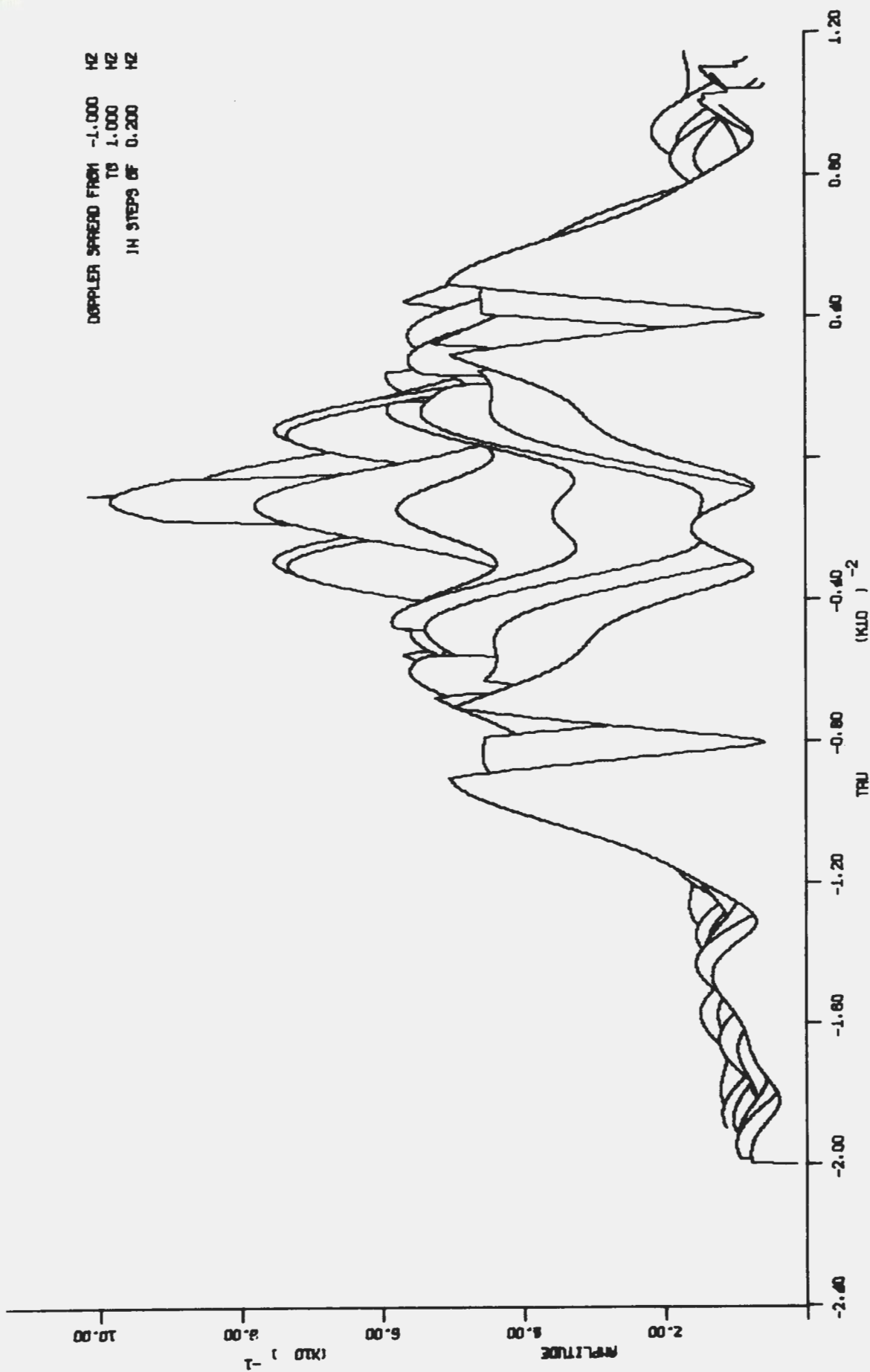


FIG. 4-9 WIDEBAND GRAPH, DELAY=.004

CHAPTER V

CONCLUSIONS

A. SUMMARY

The purpose of this thesis was to formulate an ambiguity function of a linear frequency modulated signal under both narrow-band and wideband conditions in order to investigate the effects of echo splitting. Because echo splitting is primarily a problem in underwater detection and tracking systems, representative sonar parameters were utilized. Computer-drawn plots of the ambiguity function for the case where two returning signals are received were presented.

It was suggested that when echo splitting is caused by a target exhibiting multiple reflecting surfaces due to the physical extensions of the target, there may be a possibility that the multiple returns could provide a means of target recognition. The graphical results obtained during this investigation were too limited to evaluate the effects of echo splitting on target signatures.

B. AREAS OF FUTURE STUDY

Further investigation of the wideband case appears warranted because of its particular importance to sonar systems. It would also seem profitable to investigate the effects of echo splitting on other large time-bandwidth product type signals such as Barker codes, pseudo-noise codes and complimentary codes.

BIBLIOGRAPHY

1. Cook, C. E., M. Bernfeld, J. Paolillo and C. A. Palmieri. "Matched Filtering, Pulse Compression and Wave Form Design," Microwave Journal, Vol. 7, pp. 51-64. October, 1964.
2. Woodward, P. M. Probability and Information Theory with Applications to Radar. New York: McGraw-Hill Book Co., Inc.
3. Siebert, W. M. "A Radar Detection Philosophy," IRE Trans. on Information Theory, Vol. IT-4, pp. 171-212. September, 1954.
4. Goodman, J. M. "Analysis of Matched-Filter Radar Multipath Returns at 435 MC." Naval Research Laboratory Report 5767, April 17, 1962.
5. Garber, S. M. "High Resolution Sonar Signals in a Multipath Environment," Supplement to IEEE Trans. on Aerospace and Electronic Systems, Vol. AES-2, No. 6, pp. 431-440. November, 1965.
6. Kelly, E. J. and R. P. Wishner. "Matched-Filter Theory for High Velocity, Accelerating Targets," IEEE Trans. on Military Electronics, Vol. MIL 9, pp. 56-69. January, 1965.
7. Rihaczek, A. W. "Radar Resolution of Moving Targets," IEEE Transactions on Information Theory, Vol. IT-13, No. 1, pp. 51-56. January, 1967.
8. Harris, B. and S. A. Kramer. "Asymptotic Evaluation of the Ambiguity Functions of High Gain FM Matched Filter Sonar Systems," Supplement to IEEE Trans. on Aerospace and Electronic Systems, Vol. AES-3, pp. 463-471. November, 1967.
9. Kramer, S. A. "Doppler and Acceleration Tolerance of High Gain, Wideband Linear FM Correlation Sonars," Proc. IEEE, Vol. 55, pp. 627-636. May, 1967.
10. Mitchell, R. L. and A. W. Rihaczek. "Matched-Filter Responses of the Linear FM Waveforms," IEEE Trans. on Aerospace and Electronic Systems, Vol. AES-4, pp. 417-432. May, 1968.
11. Rihaczek, A. W. "Delay-Doppler Ambiguity Function for Wideband Signals," IEEE Trans. on Aerospace and Electronic Systems, Vol. AES-3, pp. 705-711. July, 1967.
12. Remley, W. R. "Doppler Dispersion Effects in Matched Filter Detection and Resolution," Proc. IEEE, Vol. 54, pp. 33-39. January, 1966.
13. Akita, R. M. "An Investigation of the Narrow-band and Wideband Ambiguity Functions for Complimentary Codes." Master's Thesis, Naval Postgraduate School, Monterey, California, June, 1968.

APPENDIX A.

EXAMINATION OF THE NARROW-BAND AMBIGUITY FUNCTION FOR A PULSED CW SYSTEM UNDER MATCHED CONDITIONS

For $\mu=0$, Equation 2-10 can be written as

$$\psi(\tau, \omega, \Delta) = \frac{2}{T} \left| \int_{-\infty}^{\infty} \left[\alpha_1 X(t) \cos\{(\omega_0 + \omega_{d_1})t\} + \alpha_2 X(t-\Delta) \cos\{(\omega_0 + \omega_{d_2})(t-\Delta)\} \right] X(t-\tau') e^{j[\omega_1(t-\tau') + \omega_0 t]} dt \right|. \quad (A-1)$$

Consequently, $\psi(0,0,\Delta)$ can be written, with some trigonometric substitutions as

$$\begin{aligned} \psi(0,0,\Delta) = \frac{1}{T} & \left| \int_0^T \left\langle \cos(2\omega_0 t) + 1 + j \sin(2\omega_0 t) \right\rangle dt \right. \\ & + \int_{\Delta}^T \left\langle \cos(2\omega_0 t - \omega_0 \Delta) + \cos \omega_0 \Delta + j \sin(2\omega_0 t - \omega_0 \Delta) \right. \\ & \left. \left. + j \sin \omega_0 \Delta \right\rangle dt \right|, \end{aligned} \quad (A-2)$$

where

$$\alpha_1 = \alpha_2 = 1.$$

Equation A-2 can then be written as

$$\begin{aligned} \psi(0,0,\Delta) = \frac{1}{T} & \left| \int_0^T 2\cos^2 \omega_0 t dt + \cos \omega_0 \Delta \int_{\Delta}^T 2\sin^2 \omega_0 t dt \right. \\ & + \sin \omega_0 \Delta \int_{\Delta}^T \sin 2\omega_0 t dt + j \left\langle \int_0^T \sin 2\omega_0 t dt \right. \\ & \left. \left. + \sin \omega_0 \Delta \int_{\Delta}^T 2\sin^2 \omega_0 t dt \right\rangle \right|. \end{aligned} \quad (A-3)$$

If the assumption is made that there are an integral number of cycles within the envelope of the pulse,

$$\frac{n}{f} = T; n = 1, 2, \dots,$$

then considerable reduction in Equation A-3 is possible. For example,

$$\int_0^T 2\cos^2\omega_0 t \, dt = T$$

$$\int_0^T \sin 2\omega_0 t \, dt = 0.$$

As this investigation is directed at values of Δ on the order of a few milliseconds in the sonar case, the terms

$$\cos\omega_0\Delta \int_{\Delta}^T 2\sin^2\omega_0 t \, dt \approx -T\cos\omega_0\Delta^*$$

and

$$\cos\omega_0\Delta \int_{\Delta}^T \sin 2\omega_0 t \, dt \approx 0.$$

These same arguments hold for the imaginary terms and so Equation A-3 can be written as

$$\begin{aligned} \psi(0,0,\Delta) &= \left| 1 + \cos\omega_0\Delta + j \sin\omega_0\Delta \right| \\ &= \left| 1 + e^{j\omega_0\Delta} \right| \\ &= 2 \left| \cos \frac{\omega_0\Delta}{2} \right|. \end{aligned} \tag{A-4}$$

*The value of this integral will actually be slightly less, due to the process of integrating over a partial cycle and reduction by Δ .

APPENDIX B

EVALUATION OF THE WIDEBAND AMBIGUITY FUNCTION

Integration of Equation 4-14 is facilitated by investigation of the envelope terms. $X(t)$ was previously defined as

$$X(t) = u(t) - u(t-T).$$

Therefore

$$\begin{aligned} X(D't) &= u(D'\{t\}) - u(D'\{t - \frac{T}{D'}\}) \\ &= u(t) - u(t - \frac{T}{D'}). \end{aligned}$$

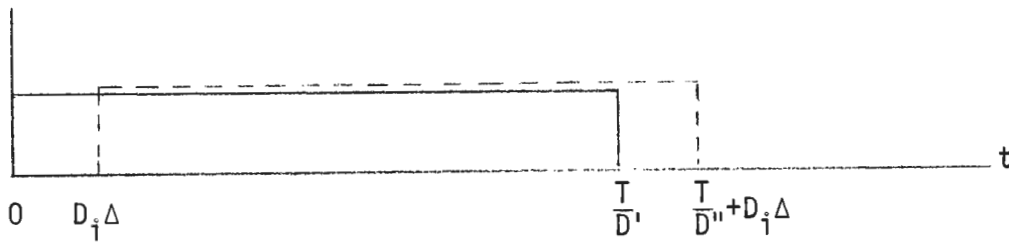
In a similar manner,

$$X(D''\{t - D_i\Delta\}) = u(t - D_i\Delta) - u(t - D_i\Delta - \frac{T}{D''})$$

and

$$X(t - \tau'') = u(t - \tau'') - u(t - T - \tau'').$$

The received envelopes can be plotted as



A step by step breakdown of the various integrals can now be presented by simply shifting the filter envelope over the range of τ'' . For clarity the amplitude of the filter envelope will be shown greatly enlarged. In addition, the time axis is not to scale. We define

$$Z_1(t) = \alpha_1 D' \cos\{\omega_0 D' t + \frac{1}{4} \mu(D't)^2\} e^{j[\omega_0 t + \frac{1}{2} \mu(t - \tau'')^2]}$$

$$Z_2(t) = \alpha_2 D'' \cos\{\omega_0 D''(t - D_i\Delta) + \frac{1}{2} \mu[D''(t - D_i\Delta)]^2\} e^{j[\omega_0 t + \frac{1}{2} \mu(t - \tau'')^2]}$$

There are four doppler dependent cases that must be examined in order to determine the exact values of the limits.

Case I. D' and D'' are both less than 1. In this case the pulses are both expanded in time by the action of doppler.

Case II. D' and D'' are greater than 1. Pulse compression has occurred in this instance.

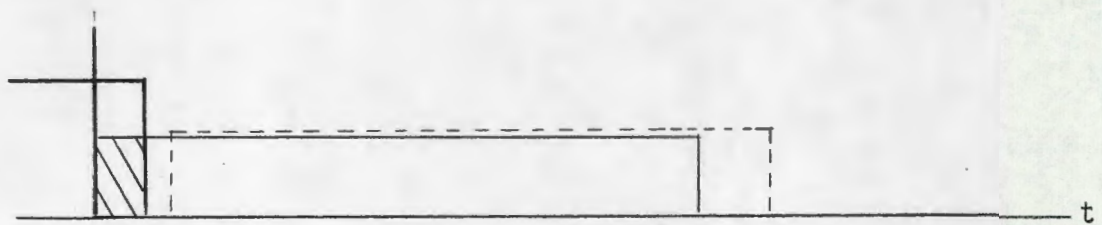
Case III. D' is less than 1, and D'' is greater than 1.

Case IV. D' is greater than 1, and D'' is less than 1.

Figure A-1 will be repeated and the relative positioning of the filter envelope will be shown to determine the proper limits in each instance.

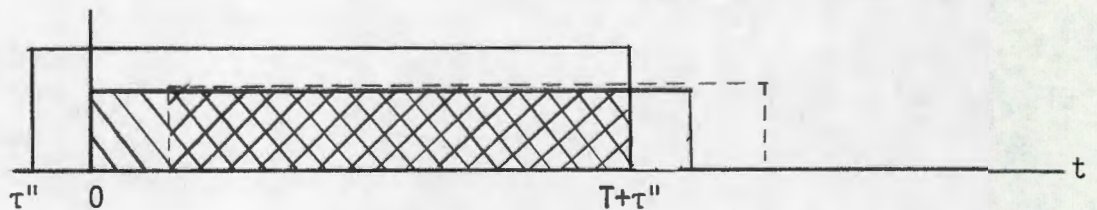
Case I.

A. $-T < \tau'' < -(T - D_i \Delta)$



$$\psi(\tau'', \omega, \Delta) = \left| \int_0^{T+\tau''} Z_1(t) dt \right|$$

B. $-(T - D_i \Delta) < \tau'' < 0$

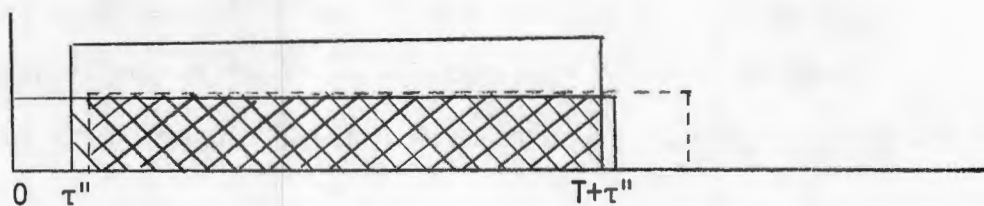


$$\psi(\tau'', \omega, \Delta) = \left| \int_0^{T+\tau''} Z_1(t) dt + \int_{D_i \Delta^2}^{T+\tau''} Z_2(t) dt \right|$$

C. Depending on the relative values of doppler, the next three integrals divide into different regions of τ'' .

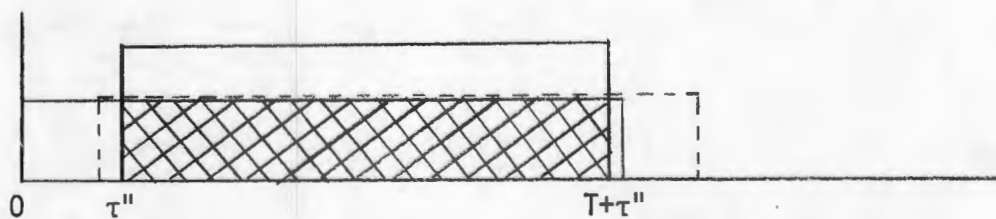
For the case where $D_1 \Delta < \frac{T}{D_1} - T$

C1. $0 < \tau'' < D_1$



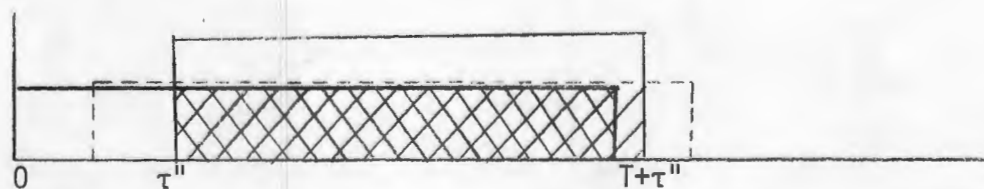
$$\psi(\tau'', \omega, \Delta) = \left| \int_{\tau''}^{T+\tau''} Z_1(t) dt + \int_{D_1 \Delta}^{T+\tau''} Z_2(t) dt \right|$$

D1. $D_1 \Delta < \tau'' < \frac{T}{D_1} - T$



$$\psi(\tau'', \omega, \Delta) = \left| \int_{\tau''}^{T+\tau''} Z_1(t) dt + \int_{\tau''}^{T+\tau''} Z_2(t) dt \right|$$

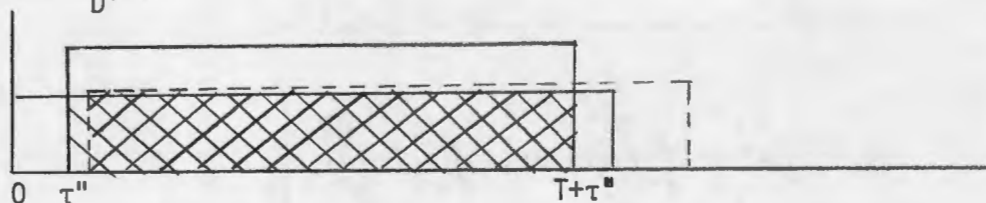
E1. $\frac{T}{D_1} - T < \tau'' < \frac{T}{D_1} + D_1 - T$



$$\psi(\tau'', \omega, \Delta) = \left| \int_{\tau''}^{T/D'} Z_1(t) dt + \int_{\tau''}^{T+\tau''} Z_2(t) dt \right|$$

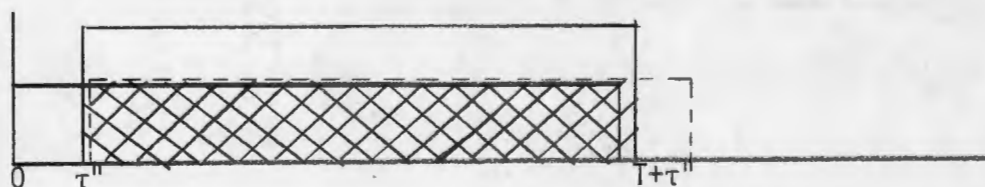
If, however, $D_i \Delta$ is greater than $\frac{T}{D_i} - T$, then the following integrals result.

C2. $0 < \tau'' < \frac{T}{D_i} - T$



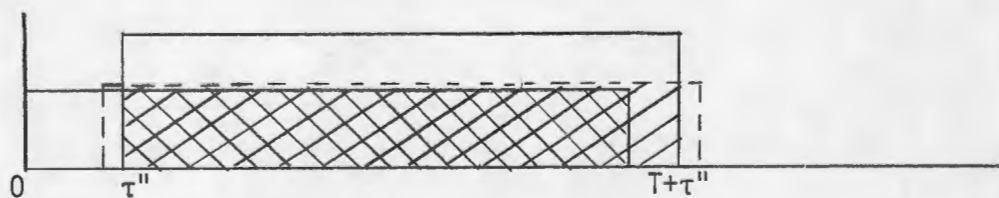
$$\psi(\tau'', \omega, \Delta) = \left| \int_{\tau''}^{T+\tau''} Z_1(t) dt + \int_{D_i \Delta}^{T+\tau''} Z_2(t) dt \right|$$

D2. $\frac{T}{D_i} - T < \tau'' < D_i \Delta$



$$\psi(\tau'', \omega, \Delta) = \left| \int_{\tau''}^{T/D'} Z_1(t) dt + \int_{D_i \Delta}^{T+\tau''} Z_2(t) dt \right|$$

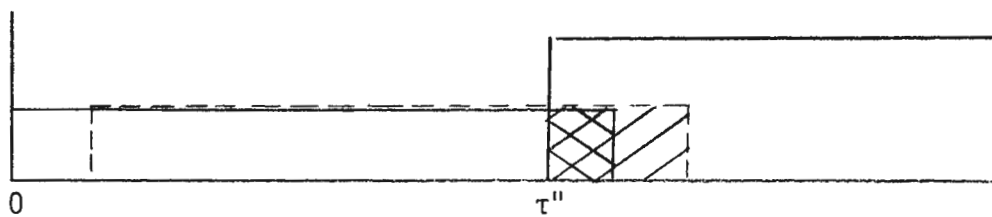
E2. $D_i \Delta < \tau'' < \frac{T}{D_i} + D_i \Delta - T$



$$\psi(\tau'', \omega, \Delta) = \left| \int_{\tau''}^{T/D'} Z_1(t) dt + \int_{\tau''}^{T+\tau''} Z_2(t) dt \right|$$

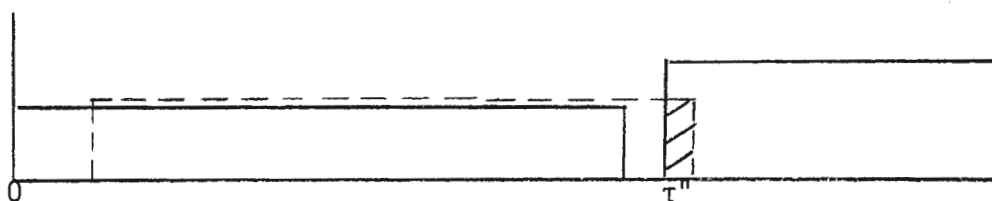
The remaining integrals in Case I do not depend on the particular value of D_i .

$$F. \quad \frac{T}{D''} + D_i \Delta - T < \tau'' < \frac{T}{D'}$$



$$\psi(\tau'', \omega, \Delta) = \left| \int_{\tau''}^{T/D'} Z_1(t) dt + \int_{\tau''}^{T/D'' + D_i \Delta} Z_2(t) dt \right|$$

$$G. \quad \frac{T}{D'} < \tau'' < \frac{T}{D''} + D_i$$



$$\psi(\tau'', \omega, \Delta) = \left| \int_{\tau''}^{T/D'' + D_i \Delta} Z_2(t) dt \right|$$

The procedure is the same in the remaining cases. Consequently, only the integral expressions resulting from investigating these limits will now be presented:

Case II.

A.	$-T < \tau'' < D_i \Delta - T$	$\psi(\tau'', \omega, \Delta) = \left \int_0^{T+\tau''} Z_1(t) dt \right $
B.	$D_i \Delta - T < \tau'' < \frac{T}{D_i} - T$	$\psi(\tau'', \omega, \Delta) = \left \int_0^{T+\tau''} Z_1(t) dt + \int_{D_i}^{T+\tau''} Z_2(t) dt \right $
$\frac{T}{D''} + D_i \Delta > T$		
C1.	$\frac{T}{D_i} - T < \tau'' < 0$	$\psi(\tau'', \omega, \Delta) = \left \int_0^{T/D_i} Z_1(t) dt + \int_{D_i \Delta}^{T+\tau''} Z_2(t) dt \right $
D1.	$0 < \tau'' < \frac{T}{D''} + D_i \Delta - T$	$\psi(\tau'', \omega, \Delta) = \left \int_{\tau''}^{T/D_i} Z_1(t) dt + \int_{D_i \Delta}^{T+\tau''} Z_2(t) dt \right $
E1.	$\frac{T}{D''} + D_i \Delta - T < \tau'' < D_i \Delta$	$\psi(\tau'', \omega, \Delta) = \left \int_{\tau''}^{T/D_i} Z_1(t) dt + \int_{D_i \Delta}^{T/D'' + D_i \Delta} Z_2(t) dt \right $
$\frac{T}{D''} + D_i \Delta < T$		
C2.	$\frac{T}{D_i} - T < \tau'' < \frac{T}{D''} + D_i \Delta - T$	$\psi(\tau'', \omega, \Delta) = \left \int_0^{T/D_i} Z_1(t) dt + \int_{D_i \Delta}^{T+\tau''} Z_2(t) dt \right $
D2.	$\frac{T}{D''} + D_i \Delta - T < \tau'' < 0$	$\psi(\tau'', \omega, \Delta) = \left \int_0^{T/D_i} Z_1(t) dt + \int_{D_i \Delta}^{T/D'' + D_i \Delta} Z_2(t) dt \right $
E2.	$0 < \tau'' < D_i \Delta$	$\psi(\tau'', \omega, \Delta) = \left \int_{\tau''}^{T/D_i} Z_1(t) dt + \int_{D_i \Delta}^{T/D'' + D_i \Delta} Z_2(t) dt \right $
F.	$D_i \Delta < \tau'' < \frac{T}{D_i}$	$\psi(\tau'', \omega, \Delta) = \left \int_{\tau''}^{T/D_i} Z_1(t) dt + \int_{\tau''}^{T/D'' + D_i \Delta} Z_2(t) dt \right $
G.	$\frac{T}{D_i} < \tau'' < \frac{T}{D''} + D_i \Delta$	$\psi(\tau'', \omega, \Delta) = \left \int_{\tau''}^{T/D'' + D_i \Delta} Z_2(t) dt \right $

INITIAL DISTRIBUTION LIST

	No. Copies
1. Defense Documentation Center Cameron Station Alexandria, Virginia 22314	20
2. Library Naval Postgraduate School Monterey, California 93940	2
3. Director of Naval Communications (OP 94) Department of the Navy Washington, D. C. 20370	1
4. Commander, Naval Security Group Command U.S. Naval Security Station 3801 Nebraska Avenue, N.W. Washington, D. C. 20390	1
5. Professor C. F. Klammer, Jr. Department of Electrical Engineering Naval Postgraduate School Monterey, California 93940	8
6. Lieutenant Francis P. Cleary 68 Elmer Road Dorchester, Massachusetts 02124	1

UNCLASSIFIED

Security Classification

DOCUMENT CONTROL DATA - R & D

(Security classification of title, body of abstract and indexing annotation must be entered when the overall report is classified)

1. ORIGINATING ACTIVITY (Corporate author) Naval Postgraduate School Monterey, California 93940		2a. REPORT SECURITY CLASSIFICATION UNCLASSIFIED	
		2b. GROUP	
3. REPORT TITLE Echo Splitting in Linear FM Doppler Ranging Systems			
4. DESCRIPTIVE NOTES (Type of report and inclusive dates) Master's Thesis			
5. AUTHOR(S) (First name, middle initial, last name) Francis P. Cleary, Lieutenant, USN			
6. REPORT DATE September 1968		7a. TOTAL NO. OF PAGES 64	7b. NO. OF REFS 13
8a. CONTRACT OR GRANT NO.		9a. ORIGINATOR'S REPORT NUMBER(S)	
b. PROJECT NO.			
c.		9b. OTHER REPORT NO(S) (Any other numbers that may be assigned this report)	
d.			
10. DISTRIBUTION STATEMENT Unclassified for public release; distribution is unlimited. Postgraduate School, Monterey, California 93940			
11. SUPPLEMENTARY NOTES		12. SPONSORING MILITARY ACTIVITY Naval Postgraduate School Monterey, California 93940	
13. ABSTRACT Echo splitting is a phenomenon that produces difficulties in estimating target range and speed for radar and sonar systems. It occurs when more than one returned pulse is received from a single target for each transmitted pulse. This thesis investigates the effects of echo-splitting distortion of a linear frequency modulated (chirp) signal. An ambiguity function is proposed for both narrow-band and wideband analysis of multiple and overlapping target returns. The double echo situation is examined in detail and equations are developed for both the narrow-band and wideband cases. Finally, using typical sonar parameters, sample computer drawn plots of these ambiguity functions are presented.			

DD FORM 1473
1 NOV 65

(PAGE 1)

S/N 0101-807-6811

UNCLASSIFIED

Security Classification

UNCLASSIFIED

Security Classification

14.

KEY WORDS

LINK A

LINK B

LINK C

ROLE

WT

ROLE

WT

ROLE

WT

Ambiguity function

Linear frequency modulation

Echo splitting

Doppler ranging systems

DD FORM 1473 (BACK)

1 NOV 65

S/N 0101-807-6821

UNCLASSIFIED

Security Classification

A-31409

1

1

1

thesC509

Echo encoding in linear FM double range

DUDLEY KNOX LIBRARY



3 2768 00421994 9

DUDLEY KNOX LIBRARY